

# Non-Axisymmetric Inflatable Pressure Structure (NAIPS) Concept that Enables Mass Efficient Packageable Pressure Vessels with Sealable Openings

*William R. Doggett, Thomas C. Jones, Winfred S. Kenner, David F. Moore,  
Judith J. Watson, and Jerry E. Warren  
Langley Research Center, Hampton, Virginia*

*Alberto Makino and Bryan Yount  
Ames Research Center, Moffett Field, California*

*Molly Selig, Khadijah Shariff, and Douglas Litteken  
Johnson Space Center, Houston, Texas*

*Martin M. Mikulas, Jr.  
National Institute of Aerospace, Hampton, Virginia*

## NASA STI Program . . . in Profile

Since its founding, NASA has been dedicated to the advancement of aeronautics and space science. The NASA scientific and technical information (STI) program plays a key part in helping NASA maintain this important role.

The NASA STI program operates under the auspices of the Agency Chief Information Officer. It collects, organizes, provides for archiving, and disseminates NASA's STI. The NASA STI program provides access to the NTRS Registered and its public interface, the NASA Technical Reports Server, thus providing one of the largest collections of aeronautical and space science STI in the world. Results are published in both non-NASA channels and by NASA in the NASA STI Report Series, which includes the following report types:

- **TECHNICAL PUBLICATION.** Reports of completed research or a major significant phase of research that present the results of NASA Programs and include extensive data or theoretical analysis. Includes compilations of significant scientific and technical data and information deemed to be of continuing reference value. NASA counter-part of peer-reviewed formal professional papers but has less stringent limitations on manuscript length and extent of graphic presentations.
- **TECHNICAL MEMORANDUM.** Scientific and technical findings that are preliminary or of specialized interest, e.g., quick release reports, working papers, and bibliographies that contain minimal annotation. Does not contain extensive analysis.
- **CONTRACTOR REPORT.** Scientific and technical findings by NASA-sponsored contractors and grantees.

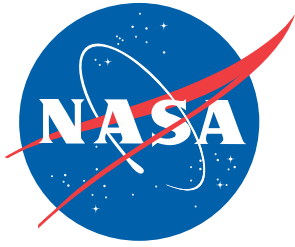
- **CONFERENCE PUBLICATION.** Collected papers from scientific and technical conferences, symposia, seminars, or other meetings sponsored or co-sponsored by NASA.
- **SPECIAL PUBLICATION.** Scientific, technical, or historical information from NASA programs, projects, and missions, often concerned with subjects having substantial public interest.
- **TECHNICAL TRANSLATION.** English-language translations of foreign scientific and technical material pertinent to NASA's mission.

Specialized services also include organizing and publishing research results, distributing specialized research announcements and feeds, providing information desk and personal search support, and enabling data exchange services.

For more information about the NASA STI program, see the following:

- Access the NASA STI program home page at <http://www.sti.nasa.gov>
- E-mail your question to [help@sti.nasa.gov](mailto:help@sti.nasa.gov)
- Phone the NASA STI Information Desk at 757-864-9658
- Write to:  
NASA STI Information Desk  
Mail Stop 148  
NASA Langley Research Center  
Hampton, VA 23681-2199

NASA/TM-2016-219331



# Non-Axisymmetric Inflatable Pressure Structure (NAIPS) Concept that Enables Mass Efficient Packageable Pressure Vessels with Sealable Openings

*William R. Doggett, Thomas C. Jones, Winfred S. Kenner, David F. Moore,  
Judith J. Watson, and Jerry E. Warren  
Langley Research Center, Hampton, Virginia*

*Alberto Makino and Bryan Yount  
Ames Research Center, Moffett Field, California*

*Molly Selig, Khadijah Shariff, and Douglas Litteken  
Johnson Space Center, Houston, Texas*

*Martin M. Mikulas, Jr.  
National Institute of Aerospace, Hampton, Virginia*

National Aeronautics and  
Space Administration

Langley Research Center  
Hampton, Virginia 23681-2199

---

August 2016

## **Acknowledgments**

The contributions described in this paper were the result of a large team effort. All contributions from the study team are gratefully acknowledged. The primary members of the team are: Lynn Bowman, Greg Dean, Sam James, George Hilton, Scott Kenner, Bonnie Lahiff, William (Mike) Langford, Vincent LeBoff, Laura Leybold, Douglas Litteken, Nathan Mesick, David Moore, Teresa Oneil, James (Jim) Phelps, Timothy (Tim) Roach, Nathaniel Mesick, Khadijah Shariff, Clarence Stanfield, Arlon Sullivan, Gerard Valle, Fred Whitehead, Thomas (Tom) Walker, and Bryan Yount.

Available from:

NASA STI Program / Mail Stop 148  
NASA Langley Research Center  
Hampton, VA 23681-2199  
Fax: 757-864-6500

## Table of Contents

1	Introduction .....	1
2	Elongated Inflatable Structure Definitions and Assumptions .....	2
2.1	Pressure Vessel Weight Equations.....	3
2.2	Zero Hoop Stress Shape .....	3
3	Elongated Pressure Vessel Concept .....	4
3.1	A. Fabrication Approach.....	5
3.2	B. Proof-of-Concept Model.....	6
3.3	C. Primary Load Cords.....	6
3.4	D. Application to Airlocks .....	7
4	Launch Packaging of the Airlock .....	7
5	Finite Element Analysis .....	8
6	Pressure Vessel Weight Performance Metrics .....	9
7	Design Robustness.....	10
8	Conclusions .....	11
9	References .....	13

## List of Figures

Figure 1. Example of an elongated, non-axisymmetric, inflatable pressure structure (NAIPS). .14	14
Figure 2. Woven straps forming filamentary pressure vessel with state of the art opening. ....14	14
Figure 3. Parachute shape relying on lobed structure to transfer load to cordage. ....15	15
Figure 4. Zero hoop stress test article developed and analyzed by Mikulas in 1970. <sup>1</sup> .....16	16
Figure 5. Typical shapes considered for elongated pressure vessel end domes. ....16	16
Figure 6. Comparison of the cross-sections of a zero hoop stress shape and sphere with the same maximum radius .....17	17
Figure 7. Schematic of a zero hoop stress shape identified by Pagitz and Pellegrino <sup>11</sup> where the individual meridional segments are in equilibrium with the internal pressure. ....18	18
Figure 8. In a zero hoop stress shape, the loads at the poles, P, must resist all the pressure load acting on the cross-sectional area.....18	18
Figure 9. Potential shapes formed from zero hoop stress shape and cylinder mid body.....19	19
Figure 10. Polar buckle to allow separation of load carrying elements at pole. ....19	19
Figure 11. NAIPS consists of two separated halves of a zero hoop stress isotenoid shape joined together by a circumferentially wrapped cylindrical section and two axial cords.....20	20
Figure 12. FEA inflation simulation sequence of an elongated airlock fabricated from two flat sheets.....20	20
Figure 13. Full-scale low surface stress polypropylene model of a NAIPS without cords. ....21	21
Figure 14. Primary load carrying cords shown on gray schematic of NAIPS.....21	21
Figure 15. Development model showing the primary load carrying cords.....22	22
Figure 16. Two views of the full-scale NAIPS airlock concept. ....23	23
Figure 17. Deployed airlock with entry transition structure from vehicle between axial cords...23	23
Figure 18. Deployed airlock with equatorial interface for entry transition structure. ....24	24
Figure 19. Packaged airlock with entry transition structure between axial cords. ....25	25
Figure 20. Folding of the seal forming hatch.....25	25
Figure 21. Packaged airlock with equatorial entry transition structure. ....25	25
Figure 22. Packaging start for equatorial hatch. ....25	25
Figure 23. FEA model of NAIPS.....26	26
Figure 24. FEA model of NAIPS superimposed upon the polypropylene model. ....26	26
Figure 25. 3/8th scale Kevlar model used to refine meridional tendon geometry.....27	27
Figure 26. Line loads in full scale 21 lobe FEA. ....28	28
Figure 27. FEA comparison of 21 lobe dome with and without mid-body lobes.....29	29

Figure 28. Weight performance metric chart enabling weight projections at different scales (SI units).....30

Figure 29. Weight performance metric chart enabling weight projections at different scales in (English units).....31

Figure 30. NAIPS with redundant cordage network.....32

Figure 31. NAIPS with redundant cordage network indexed to fabric layer.....32

**List of Tables**

Table 1. Hatch component weights. 1.02 m (40 inch) inside diameter. ....15

Table 2. Comparison of the geometric properties for a zero hoop stress shape and a sphere of the same radius.....17

Table 3. Material properties for figures 28 and 29. ....31

## Acronyms

EAM	=	exploration augmentation module
FEA	=	finite element analysis
MASH	=	minimalistic advanced soft goods hatch
NAIPS	=	non-axisymmetric inflatable pressure structure

## Nomenclature

$\gamma$	=	specific weight in units of N/m <sup>3</sup> (lbf/in <sup>3</sup> )
$\sigma$	=	breaking stress in units of Pa (lbf/in <sup>2</sup> )
$\sigma/\gamma$	=	specific strength in units of m (in)
$\sigma t$	=	stress resultant from shell theory in units of N/m (lbf/in)
$p$	=	differential pressure from inside to outside of pressure vessel (assumed > 0) in units of kPa (psi)
P	=	pole load from low hoop stress shape in units of N (lbf)
R	=	internal radius of pressure vessel in units of m (in)
R <sub>L</sub>	=	end dome lobe radius in units of m (in)
t	=	thickness in units of m (in)
V	=	volume in units of m <sup>3</sup> (in <sup>3</sup> )
W	=	weight in units of N (lbf)

## Abstract

*Achieving minimal launch volume and mass are always important for space missions, especially for deep space manned missions where the costs required to transport mass to the destination are high and volume in the payload shroud is limited. Pressure vessels are used for many purposes in space missions including habitats, airlocks, and tank farms for fuel or processed resources. A lucrative approach to minimize launch volume is to construct the pressure vessels from soft goods so that they can be compactly packaged for launch and then inflated en route or at the final destination. In addition, there is the potential to reduce system mass because the packaged pressure vessels are inherently robust to launch loads and do not need to be modified from their in-service configuration to survive the launch environment. A novel concept is presented herein, in which sealable openings or hatches into the pressure vessels can also be fabricated from soft goods. To accomplish this, the structural shape is designed to have large regions where one principal stress is near zero. The pressure vessel is also required to have an elongated geometry for applications such as airlocks. These two requirements led to the selection of a unique structural architecture that is referred to as a Non-Axisymmetric Inflatable Pressure Structure (NAIPS). The NAIPS concept is described and its structural performance is discussed in the present paper.*

# 1 Introduction

Deployable structures are used on most spacecraft to provide compact launch packaging for structures that expand into larger operational configurations once in space. Although this technology is mature for mechanically deployable spacecraft systems, the same acceptance has yet to be achieved for large filamentary inflation-deployed structures. The primary benefit achieved from soft goods structures is their ability to package compactly into a variety of shapes. Additional motivation to use soft goods structures results from the potential for mass savings achievable from three features: (1) the use of very high specific strength filamentary materials; (2) reduced design loads since the design is driven by in-space loads following deployment instead of loads induced during launch, which are typically higher; and (3) reduction in the mass of the launch shroud and launch system due to the compactness of the packaged inflatable structure. An additional benefit of a Non-Axisymmetric Inflatable Pressure Structure (NAIPS) is the ability to replace heavy, rigid, hatch openings typically associated with habitats, airlocks, and other pressure vessels with openings. The rigid hatch openings are replaced with packageable linear “Ziploc®”-like openings in low principal stress regions. An example hardware model of a NAIPS constructed from polypropylene is shown in figure 1. The NAIPS is mirror symmetric about the equator and has three distinct regions as indicated: two end domes and a mid-body.

Filamentary structures enable a variety of packaging schemes without impacting the in-situ performance. These structures fold readily, requiring few if any added design features to create folds. However, the transitions to rigid components to form openings negate the majority of the benefits of soft goods structures. Typically, to form an opening, a rigid frame is needed, as shown in figure 2. In this example, the pressure vessel is formed from a restraint layer of woven straps that encapsulate a bladder which forms the impermeable layer. The weights of the hatch components are provided in table 1. The hatch shown provides a 1.02 m (40 inch) clear opening for astronaut egress consistent with current practice. Further, current hatches scale poorly, with the loads increasing as the square of the opening size, i.e., pressure x opening area. For example, for a hatch in the side of a cylindrical pressure vessel, as the size of the opening increases, the loads in the frame increase proportional to the diameter of the opening squared. This is true of the pressure loads on the door as well as the maximum moment the frame must withstand from the distributed beam load that the frame must bridge around the opening (figure 2). In addition, in a filamentary structure with a rigid hatch, the shape and location of the hatch dictate much of the packaging of the pressure vessel. In contrast, the NAIPS enables a flexible hatch opening to be integrated into the pressure vessel, which has little impact on packaging.

Currently, there is a reluctance to use filamentary inflatable structures in space applications because they use nontraditional materials, nontraditional manufacturing techniques, and have load paths that are not precisely defined. Although modern filamentary components such as straps, cords, and fabrics possess extremely high specific strengths ( $\sigma/\gamma$ ), their use is made more difficult because they are highly nonlinear, subject to creep, and subject to imperfections created during the fabrication process. In order to capitalize on the high-performance properties of modern filamentary materials, structural concepts must be conceived to accommodate these material characteristics in a rational and robust fashion. The NAIPS is being developed to mitigate these issues using a design approach similar to that previously used for axisymmetric inflatable structures (refs. 1–8). The NAIPS is fabricated from initially flat material to simplify construction, and the primary loads are carried in cords for which the loads are simply and

robustly predictable (ref. 1). The resulting elongated pressurized NAIPS shape is achieved by capping a simple cylindrical shape with well understood nearly zero hoop stress shapes. The result is a blended body shape that is easily fabricated from readily available flat material stock and for which all major loads are well defined.

The primary inspiration for the NAIPS comes from the parachute concept and analysis originated by Sir Geoffrey I. Taylor in 1919 (ref. 2) and shown in figure 3-a. Taylor's work led to the lobed parachute design clearly visible in the recent Orion parachutes, shown in figure 3-b, where the lobes transfer aerodynamic loads to the cords. The major innovation presented is extending the axisymmetric shape of Taylor to an elongated cylinder-like shape with novel end closures. In this paper, the basic equations required to predict the resulting loads, volumes, and weights for such a shape are presented. A full-scale proof of concept model is discussed that demonstrates the feasibility of the NAIPS. Also, the deployed geometry predicted by nonlinear finite element analysis is qualitatively compared to the geometry of pressurized laboratory experimental models. Finally, a performance metric chart has been developed to highlight the available mass savings as the NAIPS is scaled and to enable NAIPS performance to be compared with alternate concepts. This performance metric chart is based on the pioneering isotensoid pressure vessel weight analysis developed by Scheurch in 1963 (refs. 3 and 4).

A major feature incorporated into the NAIPS is deep equatorial lobes that are similar to those found in parachutes. These lobes are designed so that the extremely high pressure load is directed into structurally efficient filamentary cords, allowing the stresses in the fabric to remain low. Although this concept has been used successfully for parachutes since Taylor's work in 1919, more recent work has developed and demonstrated the use of lobed structures in closed, pressurized volume decelerators (refs.5-8). Two major lessons learned from that work were (1) the importance of ensuring, through proper design, that the lobes are properly formed to keep their stresses low; and (2) that the high-load-carrying cords have sufficient stiffness to prevent undesirable stresses from being induced in the fabric lobes. Recent work has advanced the technology for such lobed structures as well as demonstrated their practicality (refs. 9-12). The major innovation of the present concept is a novel adaptation of previous work on axisymmetric lobed structures that will provide elongated, non-axisymmetric, inflatable pressure vessels for applications such as airlocks and in-space hangars which include integrated lightweight packageable openings.

## **2 Elongated Inflatable Structure Definitions and Assumptions**

The focus of the current research is to develop structural concepts to demonstrate the performance of elongated inflatable soft goods pressure vessels that can be used as airlocks in future space exploration missions. While a relatively small-volume airlock is the focus, the technology being developed is scalable to large hangars. These large hangars are still constructed from thin fabric because only the diameter of the filamentary reinforcing cords increases as the size of the structure increases. A low surface stress example of the proposed pressure vessel shape (which does not use a network of filamentary reinforcing cords) is shown in figure 1. In 1970, Mikulas (ref. 1) demonstrated that a close approximation to the theoretical zero hoop stress shape could be obtained by simply inflating a volume constructed from two flat circular membranes seamed around their circumferences, as shown in figure 4-a. The resulting shape has near zero hoop stress over the majority of the surface, as shown in figure 4-b, enabling a linear seal to be integrated without experiencing a cross load (i.e., perpendicular to the zipper

direction which is a hoop load in figure 4-b). In the present study, it has been determined that the elongated pressure vessel of figure 1 can be fabricated in a similar fashion. Alternatively, the mid body can be fabricated as a braid as described by Barido (ref. 13) or as a lobed structure as described by Williams (ref. 14). A major advantage of this new elongated design is that lower strength flexible hatches or openings can be placed in low-stress regions that naturally occur in the inflated pressure vessel. This design is in stark contrast to that of traditional pressure vessel designs where conventional rigid hatches and openings introduce geometric discontinuities that result in large local stresses. The combination of an inflatable soft goods pressure vessel with a flexible hatch results in a low mass airlock that can be stowed into various compact configurations to suit many different mission architectures.

## 2.1 Pressure Vessel Weight Equations

Structures that take advantage of low-stress regions have been in use since 1919 in the form of parachutes (ref. 2, figure 3) and high altitude balloons (ref. 1). In the early 1960s, Scheurch showed (refs. 3 and 4) that families of shapes exist called “isotensoids,” where all filamentary material is fully loaded, are capable of being tailored to take advantage of the material’s high specific strength. From this work, Scheurch derived the simple expression in equation (1) for the weight of an isotensoid pressure vessel:

$$W = 3 \frac{pV}{\sigma/\gamma} \quad (1)$$

where,  $W$ , is the weight of the filaments required to carry the internal pressure,  $p$ , for a given volume,  $V$ , and  $\sigma/\gamma$  is the specific strength of the filaments (the breaking stress,  $\sigma$  divided by the specific weight,  $\gamma$ ). The isotensoid design is used as the point of departure for conceiving the current structural concept where the major loads are carried by a network of tension cords that lie along well defined principal load paths. As with parachutes, the pressure is resisted by low stress, lobed fabric material that transfers load into a highly efficient network of reinforcing cords. For comparison with equation (1), the weight of a spherical pressure vessel fabricated from isotropic materials is:

$$W = \frac{3}{2} \frac{pV}{\sigma/\gamma} \quad (2)$$

A spherical pressure vessel is the most efficient shape for an isotropic material. Although it appears from equation (2) that the isotropic pressure vessel has half the weight of the isotensoid pressure vessel, as given by equation (1), the advantage of filamentary structures results from the fact that the material specific strength,  $\sigma/\gamma$ , can be four or more times greater than the specific strength of isotropic materials, as will be discussed in section 5. This results in filamentary structures that are half the weight or less than corresponding metallic isotropic structures.

## 2.2 Zero Hoop Stress Shape

According to linear shell theory, the distribution and values of the stresses in a pressure-loaded structure can be controlled through changes in the initial shape. For the sphere shown in figure

5a, the stresses are equal in all directions. This feature makes a sphere an ideal choice for isotropic materials, such as metals that have significant stiffness and strength in two perpendicular directions. However, a sphere is not the best design choice for filamentary structures that only have significant strength and stiffness in one direction per filament layer. Since compact packaging of the pressure structure is a fundamental design objective, the use of flexible filamentary materials is desirable because the resulting structure readily accommodates folding into a compact packaged state. For these materials, isotenoid shapes like the one shown in figure 5b and defined by Scheurch (refs. 3 and 4) are the best choice. Although these ideal isotenoid shapes have met with success for relatively small pressure vessels, their fabrication becomes impractical for large pressure structures such as parachutes or decelerators. Instead, parachutes use a deeply lobed fabric structure reinforced with filamentary cords. The resulting deformed shape of the network of filamentary reinforcing cords closely approximates the shape of the highly efficient isotenoid structure. The major advantage for such lobed shapes is that they are simple to fabricate by attaching a network of filamentary cords to initially flat fabric.

Structures that are well suited to the use of high strength-to-weight ratio filamentary materials are those that have a zero, or nearly zero stress in one direction (refs. 1 and 2). Although this shape has been commonly analyzed and used in parachutes, the zero hoop stress shape can also form a wide variety of closed pressure vessel shapes (ref. 14). A common feature of all of these shapes is that they are axisymmetric.

The basic cross-section of an ideal zero hoop stress shape, based on linear theory, is shown in figure 6, where the zero hoop stress shape is inscribed within a spherical cross-section. The equations for the circumference, cross-sectional area, surface area and volume of the two shapes are presented in table 2. The geometry of a typical lobed axisymmetric low hoop stress pressure structure is shown in figure 7. Each of the individual lobed meridional segments shown in figure 7 is in equilibrium with the internal pressure (ref. 12) with no resulting hoop stress at the segment boundary. Similarly, for a zero hoop stress shape, the result of having such a geometry is to create concentrated loads at the poles, as shown in figure 8, where the load at each pole, top and bottom of the figure, is half of the cross sectional area times the internal pressure. Because the hoop load is zero, there are no other loads present perpendicular to the cross section boundary.

### **3 Elongated Pressure Vessel Concept**

A variety of potential elongated pressure vessel shapes were evaluated in order to identify concepts capable of efficiently supporting flexible packageable hatch openings. An elongated pressure vessel was selected over a scaled-up version of the zero hoop stress shape, shown in figure 4, because the volume required to enclose two astronauts is much lower, thereby reducing the amount of atmospheric gases necessary to support airlock operations. Two of the most promising shapes are formed by appending half of a zero hoop stress shape to each end of a cylinder, where the zero hoop stress shape is formed by cutting along either a polar or equatorial plane, as shown in figure 9. When an equatorial cut is appended to a cylinder, as shown in the upper right of figure 9, the convergence of the loads at the pole of the zero hoop stress shape presents several difficulties not found when a polar cut is appended to a cylinder, as shown in the lower right of figure 9. The first difficulty with the equatorial cut is that it limits the regions of low stress. First, the size of the opening is limited to approximately half of the cylinder diameter because the opening is constrained to lie along a meridian direction line from the equator to the

highly stressed polar region, as shown in the upper right of figure 9. The opening size can be increased by developing a method for separating and rejoining the load carrying structural elements at the pole. However, this will likely require rigid hardware, such as that shown in figure 10, that is not conducive to efficient packaging and more importantly adds additional steps to opening and closing the air-lock. Secondly, there are no large regions of low stress in the mid-body due to the presence of axial direction cords uniformly spaced around the circumference of the cylindrical mid-body. These cords carry large tension loads and prevent introduction of a circumferential opening in the cylindrical mid-body. Neither of these difficulties are present in the polar cut zero hoop stress concept shown in the lower right of figure 9, which led to the selection of this concept, hereafter referred to as a Non-Axisymmetric Inflatable Pressure Structure (NAIPS).

The objective of the research reported in the present paper is to extend the advantages afforded by lobed axisymmetric zero hoop stress structures to a NAIPS. The resulting concept is a lightweight filamentary pressure vessel that can accommodate flexible hatch openings located in low-stress regions in the end domes and mid-body. In the end domes, the meridian direction load is carried by meridional reinforcing cords and the hoop load is low near the reinforcing cords. This enables a flexible pole-to-pole meridional opening to be placed along any of the meridian direction cords. The axial load in a typical internally pressurized cylinder is caused by pressure loads on the end caps. In the NAIPS architecture, the end cap load is concentrated at the poles and carried by cords, which virtually eliminates axial load in the mid-body fabric. Therefore, the NAIPS architecture allows flexible openings to be placed in the mid-body or polar cut end domes, depending upon the desired application.

### **3.1 A. Fabrication Approach**

To fabricate an elongated NAIPS shape, two halves of the polar cut zero hoop stress shape are joined at each end of a cylinder-like mid-body structure, as shown in figure 11. As already discussed, a variety of potential shapes were evaluated and the shape shown in figure 11 was selected because it provides large uninterrupted low-stress zones that are ideal locations for large flexible openings. After numerous unsuccessful attempts, the desired shape was successfully fabricated using an approach similar to that used for parachute fabrication. Two flat fabric patterns of the desired shape were joined around the periphery and then pressurized, as shown in the finite element analysis (FEA) sequence included in figure 12. Although the three shapes shown in figure 11 appear to be geometrically incompatible, the out-of-plane compliance of the filamentary material enables the two initially flat sheets to inflate into the blended body shape, as shown in the sequence of figure 12. The resulting shape retained much of the desired low-stress regions, as indicated by the wrinkle pattern visible in figure 13-a. Thin membranes can only support tensile loads and buckle or wrinkle when trying to resist compressive loads. Thus, the wrinkles are an indication of the low/zero stress perpendicular to the wrinkle direction. As indicated by the dark lines in figure 11, cords are added in the primary load directions. Meridional cords are added to the zero hoop stress domes to off-load the fabric and axial cords are added to the cylindrical section to carry the large loads concentrating at the poles of the domes. Because the axial load is concentrated in the axial cord, the cylindrical section is fabricated with a fabric that is composed primarily of circumferential filaments to carry the hoop pressure load. The exact cord configuration is being refined to the appropriate shape using experimental models and finite element analysis.

### 3.2 B. Proof-of-Concept Model

An extensive testing program, involving a series of reduced-scale and full-scale models, is underway to further verify and understand the NAIPS shape. A side view and a perspective view of the first large scale hardware model constructed from polypropylene (figure 1) are shown in figures 13-a and 13-b, respectively. The resulting relatively smooth blended body shape is enabled by excess material in certain regions being taken up (or gathered) in the form of wrinkles that can be seen around the model. The end domes largely retain the characteristics of the zero hoop stress shape, and the blended cylindrical shape is unwrinkled on the top and bottom with wrinkles along the sides. The pattern of vertical wrinkles is seen to completely encompass the equator of the pressure vessel in figure 12 and these wrinkles represent low-stress regions that can be used to introduce flexible lightweight linear “Ziploc®”-like hatch openings. This initial model did not include reinforcing cords, but for all subsequent models, the single axial cord shown in figure 11 is replaced by double axial cords at the top and bottom of the cylinder, as shown in figures 14 and 15. This configuration was chosen to ease integration of the meridional cords while facilitating load transition between the two zero hoop stress domes. The dual cords across the mid-body have the added benefit of providing greater lateral bending stiffness for the NAIPS configuration, to counteract disturbances such as impulse loads from station keeping.

### 3.3 C. Primary Load Cords

Although the geometry formed by the initial low-surface stress demonstration model shown in figures 1 and 13 appears to be promising, it is necessary to introduce high-strength cords into the design to carry the primary loads induced by the design pressure for an airlock configuration. The design objective is to reduce the fabric stress by transferring load to the cords, allowing a lightweight easily foldable fabric to be used. The stress resultant, or running load, in the end dome fabric is given conservatively by equation (3) where  $p$  is the differential pressure from the inside to the outside of the pressure vessel, and  $R_L$  is the radius of a typical lobe (which is the primary design variable). For a specified NAIPS size,  $R_L$  and the corresponding running load are adjusted by varying the number of meridional cords:

$$\sigma t = p R_L \quad (3)$$

For the selected cord arrangement shown in figure 14, the end dome meridional cords are connected to an axial cordage loop that extends across the top and bottom of the cylindrical mid-body, transferring the primary axial loads between the end domes. High-strength circumferential fabric is required around the cylindrical mid-body section to carry the hoop pressure load. A scale model was fabricated with these cords in place and is shown in figure 15. The deep lobes on the end domes are created by properly shortening the cords relative to the initially flat material. Although this process is currently done on an iterative trial and error basis, an effort is underway to formalize the process. The deep lobes are an indication that the internal pressure load is being transferred to the cords, and that the resulting fabric hoop stresses near the cords are low because the radius of the lobes is small (ref. 10). To minimize the surface stress in the fabric, Pagitz and Pellegrino (ref. 9) showed that the lobes should be fully formed, which means the fabric approaches the cords tangent to a line from the pole through the edge of the cords. This ideal case is difficult to achieve in practice, but the shape of figure 15 is sufficiently close to the ideal case to realize the majority of the load transfer benefit.

### 3.4 D. Application to Airlocks

Two depictions of a full-scale NAIPS airlock are shown in figure 16. For this airlock concept, the hatch opening is planned to be installed in a low hoop stress area in one of the end domes. The low-stress area is perpendicular to the opening and the stress is low enough that a “Ziploc®”-like seal can be used to close the hatch opening. Several commercially available “Ziploc®”-like seals that are used for underwater applications are being studied, and different seals can withstand different magnitudes of stress across the seal. The stress across the seal can be tuned to suit a particular seal design by using equation (3) and varying the total number of lobes, which changes the lobe radius. With the airlock in an unpressurized state, the “Ziploc®”-like seal will be opened and the hatch folds back in an accordion-like fashion for astronaut egress and ingress, as shown in figure 16-b.

## 4 Launch Packaging of the Airlock

The major benefits of inflatable fabric pressure vessels, as compared to fixed volume pressure vessels, are significantly reduced packaging volumes and the ability to reconfigure the packaged shape. An inflatable fabric pressure vessel has a large number of potential packaged configurations because the fabric structure naturally accommodates folding and rolling to either form a small compact unit for launch, or to be reconfigured to accommodate unconventional packaging geometries for integration into the launch stack. The packaging scheme is tightly linked to the end-application. As an example, an airlock structure attached to a notional Exploration Augmentation Module (EAM) will be used to illustrate the packaging versatility of the NAIPS concept. Two notional options are depicted in figures 17 and 18. As discussed earlier, a hatch opening can be placed in a variety of low-stress locations, but the configuration shown in figure 16-b is used for both options described here. In figures 17 and 18, the hatch is indicated in green and is located in the same location relative to the axial cords. In figure 17, the spacecraft interface structure, which connects the airlock to the EAM and provides entry into the airlock, is located between the axial cords, and the airlock is oriented with its long axis perpendicular to the long axis of the EAM. Alternatively, in figure 18 the spacecraft interface structure is located in the middle of the barrel section of the airlock, along the equatorial region, and the airlock is oriented with its long axis parallel to the long axis of the EAM. Many design variables must be traded to optimize the orientation of the airlock, spacecraft interface structure, and location of the hatch, including ease of ingress and egress from the airlock, length of the airlock transition structure, loads on the airlock transition structure, loads on the airlock, integration of support structure for the deflated configuration, micro-meteoroid and orbital debris configuration, and integration within the launch stack. A discussion of these factors and how to trade them to optimize a configuration is beyond the scope of this paper. Instead, subsequent discussions will focus on the design versatility enabled by the NAIPS technology.

The deployed airlock of figure 17 can be packaged by wrapping it around the EAM, as depicted in figure 19. Where handholds or obstructions are present, suitable padding may be required to prevent abrasion damage from vibration during launch. The hatch seal, shown in figure 17, must be folded to allow the airlock to lie against the vehicle, as shown in figure 19. The hatch seal will have a finite bend radius and the fold will need to be supported, as depicted in figure 20, where it is shown wrapped around a support tube. The launch restraint system, such as a cordage net or straps that would be required to secure the airlock to the EAM is omitted from figure 19. This configuration is very attractive, in terms of minimizing the volume added to a launch stack,

because the airlock lays in the dynamic envelope between the EAM and launch shroud. This method of packaging minimizes the overall thickness of the packaged airlock, but has the potential to require additional padding to prevent damage from protrusions along the EAM exterior. In contrast, figure 21 depicts a packaging arrangement for the airlock configuration of figure 18. Here, the airlock has been packaged into the cavity around the spacecraft interface structure. To begin this packaging approach, the airlock is flattened, followed by straightening (to the degree possible) the linear hatch and then z-folding the end domes to form the shape shown in figure 22. The second step is then to compress this folded material around the spacecraft interface structure where it can be secured producing the packaged shape shown in figure 21. An advantage to this scheme is that the bend radius of the packaged seal is much larger and no support material is required. The resulting launch package is thicker, but it packages conveniently around the transition structure. The two packaging approaches shown in figures 19 and 21 illustrate the versatility in packaging options available with a fabric structure pressure vessel. There are a large number of alternative packaging schemes available which vary the packaged thickness and package footprint between the two approaches described.

Both approaches to packaging support straightforward deployment by pressurizing the airlock through the spacecraft interface structure. The package in figure 20 lifts off the vehicle immediately as inflation gases enter the airlock and rapidly transitions into the deployed state shown in figure 17. Deployment from the packaged state of figure 21 to the deployed state of figure 18 is envisioned to be staged. The first stage inflates the central portion of the airlock to lift the unit off the EAM, followed by release and deployment of the fabric end domes.

## 5 Finite Element Analysis

One of the goals of the Minimalistic Advanced Soft goods Hatch (MASH) project is to build upon the work by Adler and Pagitz (Refs. 9, 12), and demonstrate that FEA can be used to predict the behavior of the NAIPS restraint layer. The restraint layer is composed of the fabric and cords, and restrains expansion of the internal impermeable bladder layer during pressurization. Top and side views of the inflated geometry predicted by FEA of an unreinforced NAIPS are shown in figures 23-a and 23-b. Figure 24 is a qualitative comparison of the FEA and experimental models formed by superimposing the inflated side view of figure 23-b on top of a side view of the polypropylene model from figure 13. The overall shape predicted by the FEA closely approximates the shape of the demonstration model. The FEA also predicts wrinkles similar to those shown in figures 1 and 13.

Recently, a 3/8th scale model has been fabricated using Kevlar, as shown in figure 25. The 3/8th scale model is being used to refine the geometry of the meridional cords. As mentioned earlier, the purpose of the reinforcing cords is to carry the large meridian loads at the ends of the airlock. The most desirable position of the axial loop is shown on the right end of the model shown in figure 25-b. In this configuration, the diameter of the axial loop reduces pillowing inside of the axial cord around the pole to approximately the same radius of curvature as the meridional lobes at the equator in the end domes, while providing a reasonable bend radius of the axial cord. As the meridional cords are shortened, undesirable stresses at the cylinder-to-end dome transition develop that are difficult to model with FEA. The length of the cords will be tuned to avoid this behavior in future test specimens. Based on experience with the 3/8th scale model, a full-scale airlock with 21 lobes has been modeled and analyzed using FEA. A plot of the mid-body axial and end dome hoop line loads is shown in figure 26-a. As desired, the line loads are low and do

not appear to be influenced by the presence of the cords. A plot of the mid-body hoop and radial line loads is shown in figure 26-b. As expected, the resultants in the fabric beneath the cords is low which indicates that the cords are carrying the majority of the meridian direction load. Both of these results are consistent with simplified analytical predictions and the general design philosophy for the packageable airlock, and indicate that it is feasible to integrate a linear seal into the pressure vessel during the next phase of development. In the interim, a full scale test specimen without a linear seal is under fabrication and will be tested to generate information for comparison with the FEA results.

As mentioned earlier, the hoop direction stresses in the mid-body are large and require a filamentary material with high strength in the hoop direction. As the airlock geometry is scaled-up, the stresses become correspondingly larger and it might not be possible to find a filamentary material with enough strength to satisfy the qualification requirements. In addition, the highly biased fabric presents seaming challenges during fabrication. To enable fabrication of large scale airlocks from readily attainable nearly balanced fabrics, FEA was used to investigate the addition of hoop cordage grommets in the mid body, as shown on the right side of figure 27. The result is a lobed mid-body structure similar to that described by Williams (ref. 14) where the hoop cords carry most of the hoop loading instead of the fabric. The plots on the left side of figure 27 have been reproduced from figure 26 to ease comparison between the two designs. The majority of the low-stress zone has been maintained, as shown in figure 27-a, and the desired significant reduction in line load perpendicular to the axial cordage loop is shown in figure 27-b. In addition, there is a desirable reduction in the axial load between the axial cords in the center of the mid body, as shown in figure 27-a. These results indicate that it is possible to use relatively low-strength, balanced broad cloth fabric throughout the airlock by supporting the fabric with a cordage network that includes end dome meridional cords, axial cords, and mid body hoop cords.

Thus far, finite element modeling has produced results that are qualitatively similar to those from analytical predictions and demonstration models. This work forms the basis for future correlation studies between more detailed finite element models and data measured from actual airlock test articles. Successful correlation in these studies is important because future implementations of the airlock will most likely have different configurations and dimensions, and the ability to use FEA as a reliable analysis tool will reduce the amount of testing required to create and validate a new design.

## **6 Pressure Vessel Weight Performance Metrics**

The purpose of this section is to provide weight performance trends for the NAIPS concept. The focus is on a general understanding of the potential benefit from a NAIPS architecture at different scales, not on a detailed design for a particular application. To support this insight, the performance trends are based on a fully stressed or minimum gage design of the deployed system. These are generally not the limiting load cases in a point design due to other factors such as launch loads, but they do represent the ideal case which is a system whose design is governed by the in-service loads. In 1963, Hans Scheurch (refs. 3 and 4) developed the concept of an isotensoid pressure vessel; one in which all of the load carrying members are fully stressed, which results in the theoretically lowest weight design. The lower weight limit for a filamentary isotensoid pressure vessel is given by equation (1). This equation is plotted as the solid blue line in figures 28 and 29 for an isotensoid pressure vessel, using the Vectran material properties given

in table 3. The metric chart in figure 28 is in SI units, while the metric chart in figure 29 is in English units. It is important to realize, as discussed by Scheurch (ref. 3), that the shape with minimal theoretical weight is not unique. In fact, there are numerous such shapes that have the same weight. Most small isotensoid pressure vessels possess an axisymmetric, pumpkin-like shape that is produced by filament winding over a mandrel. This production method is impractical for larger space flight pressure vessels that are being designed to achieve compact packaging, because of the high fabrication costs. In the present paper, alternate materials and fabrication methods are discussed and the performance metric chart is used to track the weight performance of various options.

The blue dashed line shown in figures 28 and 29 represents the isotensoid weight of a pressure vessel fabricated from Vectran ( $\sigma/\gamma = 102 \text{ km}$  ( $4 \times 10^6 \text{ inches}$ )) with a surface-area-based weight penalty added to account for a bladder as well as the minimum gage fabric required to produce the lobed domes. The weight penalty was applied by adding a material with thickness 0.3 mm (0.012 inches) and a specific weight of 11 kN/m<sup>3</sup> (0.04 lb/in<sup>3</sup>). The solid black line represents an elongated aluminum pressure vessel, formed by joining two semi-spherical end-domes to a cylindrical mid-body, of the same aspect ratio as the NAIPS (i.e., with the length 2.5 times the radius). The upper right portion of the aluminum curve is constructed based on 572 MPa (83,000 psi) stress limited designs, while the lower left portion is constructed based on a minimum gage aluminum design having a wall thickness of 1.54 mm (0.06 inches). This minimum gage value was selected to show the effect of limiting material thickness during manufacture, and it is anticipated that the minimum gage used in a detailed design will differ. The strength limit of 572 MPa (83,000 psi) was selected because it corresponds to the approximate ultimate strength of 7075-T6, an aerospace grade aluminum alloy. To generate these curves, the design pressure for the filamentary Vectran pressure vessel was assumed to be 105 kPa (15.2 psi) multiplied by a factor of safety of four (the current standard required for in-space inflatable structures: see table 6 ref. 15) while the design pressure for the aluminum pressure vessel was assumed to be 105 kPa (15.2 psi) multiplied by a factor of safety of two (the current standard for in-space metallic pressure vessels: see table 5 ref. 15). Note that the specific strength of aluminum ( $\sigma/\gamma = 21 \text{ km}$  ( $8.3 \times 10^5 \text{ inches}$ )) is 1/5<sup>th</sup> that of Vectran. Therefore, as experience is gained with filamentary materials like Vectran, the factor of safety can be reduced to be more consistent with well understood metallic materials leading to an opportunity for further reduction in system weight.

Although highly reduced packaging volume is the major benefit being pursued with the development of fabric pressure vessels, launch weight is also an important factor. In figures 28 and 29, the approximate  $pV$  (pressure times volume) range for airlocks is shown by the red shaded area, while the approximate  $pV$  range for habitats is more than an order-of-magnitude higher and is indicated by the yellow shaded area. For the assumed parameters used in this preliminary study, fabric airlocks show a potential reduction in weight by a factor of  $\sim 4$  for the airlock range and a factor of  $\sim 2$  for the habitat range. Since this is a preliminary study, it is understood that additional factors are quite likely to change these initial weight estimates, but the trends are clear from the metric charts. The major point to be made here is that fabric pressure vessels will provide a significant reduction in launch volume and also provide weight savings.

## 7 Design Robustness

It is straightforward to make the restraint network redundant. Up to this point, a single axial loop is used on each side of the airlock, as shown in the 3/8th Kevlar Model (figure 25). Failure of

one these loops, which carry the axial load through the mid-body, will cause catastrophic failure of the entire structure. To alleviate this single line of failure, two axial loops can be used on each side of the airlock, as shown in figure 30, with each attached to half of the meridonal cords (figure 30-c). In figure 30-c, approximately half of the meridonal cords, shown in red, transfer load to the red axial cord loops, while the rest of the axial cords, shown in green, transfer load to the green axial cord loops. In this manner, under normal operation, each axial loop cord experiences approximately half of the axial load (i.e., their design load); however, should one axial cord fail, the remaining axial cord loop will be subject to the full axial load (i.e., their design load). Notice that should an axial cord fail, the axial cord is loaded by approximately half of the meridonal cords, with the others going slack. Thus, as the axial cords must be designed to take the entire axial load, the meridonal cords must be designed for this condition as well. Thus, the meridonal cords are also redundant, because loss of any one meridonal cord will not exceed this design case.

The geometry of the restraint cordage network relative to the broad cloth fabric layer is critical to the proper function of the NAIPS. “Indexing” (loosely sewn connections, belt loops, etc.) is used to enforce proper geometry, as shown in figure 31. In the figure, axial and meridional belt loops enforce the desired uniform distribution of the cordage network at the end-domes, and the separation of the axial cords, as shown. As discussed in section 3, the design objective is to use the cordage network to carry the predominate loads, with the restraint fabric transferring load to the cords. For example, in the end-domes, the aim is to have the cords loaded radially from the poles, while the fabric is loaded perpendicular to the cords and is not subjected to the radial load. To enforce this relationship, it is desirable to have wrinkles in the fabric perpendicular to the cords, thus preventing the fabric from building load parallel to the cords. The second purpose of the indexing is that fabric can be collected between belt loops, forming the desired wrinkle pattern, and then the belt loops are lightly sewn to the meridonal cords to hold this relationship until pressurization. As pressure builds, friction takes over to provide the predominate force between the fabric and cordage network.

## 8 Conclusions

A novel Non-Axisymmetric Inflatable Pressure Structure (NAIPS) is being developed that will provide highly compact and lightweight options for packaging large pressurized volumes for space exploration applications. The approach for developing the concept adapts highly successful technology that has been used for parachute design for almost a century to the formation of pressurized elongated shapes. Specifically, the elongated pressure vessel consists of two fabric zero hoop stress shape end domes joined together by a fabric cylindrical section, all of which is reinforced by a cordage network. The resulting unique NAIPS shape has large low-stress regions in the mid-body and end domes perpendicular to the cords. These low-stress regions are prime locations for locating novel compact, lightweight and packageable “Ziploc®”-like openings for airlock and hangar applications. This aspect of the NAIPS architecture is very important because existing soft goods concepts require rigid hatches and inserts that are heavy and prevent compact packaging.

To demonstrate the feasibility of the NAIPS, an airlock system is being developed, and several hardware models have been successfully fabricated and evaluated. These models have shown that elongated, blended body shapes can be achieved that exhibit the desired structural characteristics. Design of these initial models was guided by nonlinear finite element analyses

capable of simulating the inflation process of the relatively complex blended body shapes. As shown, it is straightforward to eliminate single point failures of the restraint cordage network without the addition of rigid elements or significantly affecting packaging volume. Finally, a performance metric chart has been developed from which the theoretical lower weight limit of a given volume pressure vessel can be obtained for a specified material system. This chart will be used to help evaluate and guide NAIPS design work. The metric chart also indicates there is potential for weight savings as compared to conventional rigid structures, with a factor of ~4 reduction in weight for airlock size pressure vessels and a factor of ~2 reduction for habitat size pressure vessels.

## 9 References

1. Mikulas, M. M., Jr., "Behavior of Double Curved Partly Wrinkled Membrane Structures Formed From an Initially Flat Membrane," Ph.D. Dissertation Virginia Polytechnic Institute, June 1970.
2. Taylor, G. L., "On the Shapes of Parachutes," (Paper written for the Advisory Committee on Aeronautics), in *The Scientific Papers of G.I. Taylor* (1963) (edited by G.K. Batchelor), Vol. 3, Cambridge University Press, Cambridge, originally written 1919.
3. Scheurch, H., "Analytical Design for Optimum Filamentary Pressure Vessels," AIAA Launch and Space Vehicle Shell Structures Conference, AIAA Paper 2914, 1963.
4. Scheurch, H., "Isotensoid Structure," US Patent 121451, February 18, 1964.
5. Houtz, N. E., "Optimization of Inflatable Drag Devices by Isotensoid Design," Paper 64-437, AIAA, 1964.
6. Fralich, R. W., Mikulas, M. M., Jr., and Robinson, M. P., "Design Information for Attached Inflatable Decelerators," LWP-469, August 31, 1967.
7. Mikulas, M. M., and Bohon, H. L., "Development Status of Attached Inflatable Decelerators, *Journal of Spacecraft and Rockets*," Vol 6, 1969.
8. Willis, C. M., and Mikulas, M. M., Jr., "Static Structural Tests of a 1.5-Meter-Diameter, Fabric Attached Inflatable Decelerator," NASA TN D-6929, 1972.
9. Pagitz, M., and Pellegrino, S., "Buckling Pressure of Pumpkin Balloons," *International Journal of Solids and Structures*, 2007.
10. Lennon, Andrew, and Sergio Pellegrino, "Structural mechanics of lobed inflatable structures," *Spacecraft Structures, Materials and Mechanical Testing 2005*, Vol. 581, 2005.
11. Lennon, A., and de Jong, M., "Geometric Analysis for Inflatable Space Habitats," *International Conference on Textile Composites and Inflatable Structures, Structural Membranes 2007* E. Oñate, and B. Kröplin, (Eds) CIMNE, Barcelona, 2007.
12. Adler, Aaron, and Mikulas, Martin, "Application of a Wrinkled Membrane Finite Element Approach to Advanced Membrane Structures," AIAA Space 2001 – Conference and Exposition, Albuquerque, NM; 28–30 August 2001.
13. Barido, Richard, et al., "Breadboard Development of the Advanced Inflatable Airlock System for EVA," No. 2003-01-2449. SAE Technical Paper, 2003.
14. Williams, Jerry G., "Development of an Expandable Airlock Utilizing the Elastic Recovery Principle (Expandable Space Station Airlocks Utilizing Stored Potential Energy from Strained Foam Material)," 1966, (1965): 467-496.
15. Design, Structural. "Test Factors of Safety for Spaceflight Hardware." NASA Technical Standard NASA-STD-5001, NASA/Marshall Space Flight Center (2008).

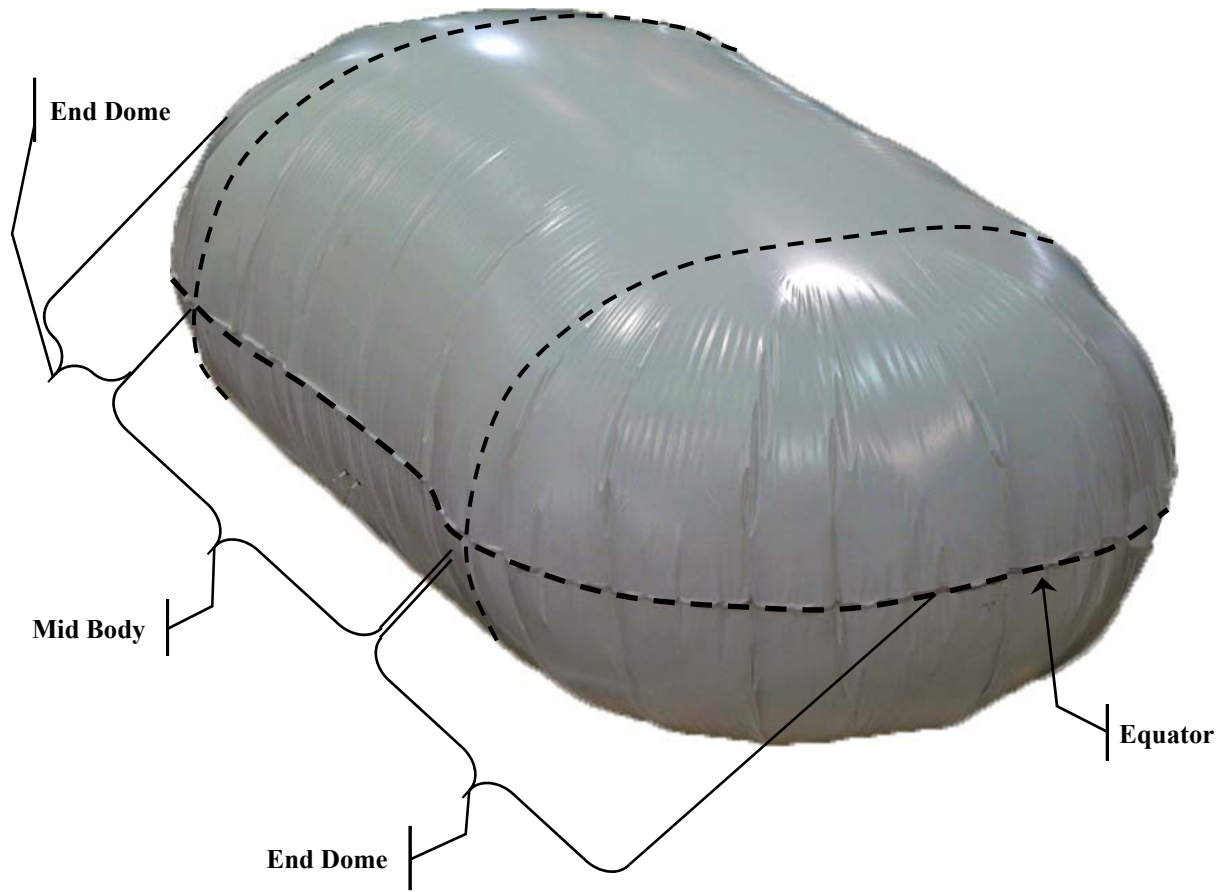


**Figure 1. Example of an elongated, non-axisymmetric, inflatable pressure structure (NAIPS).**

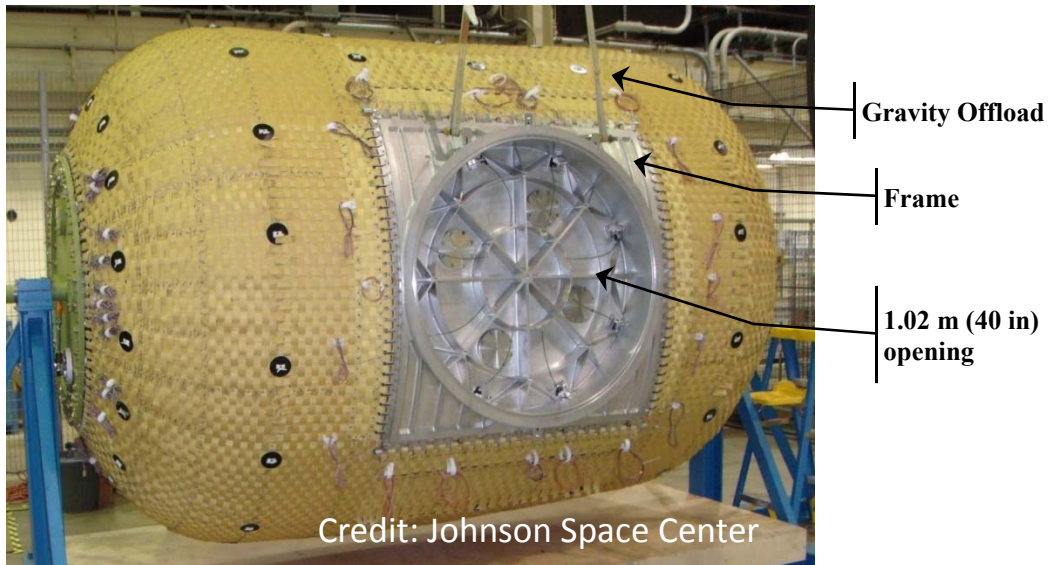
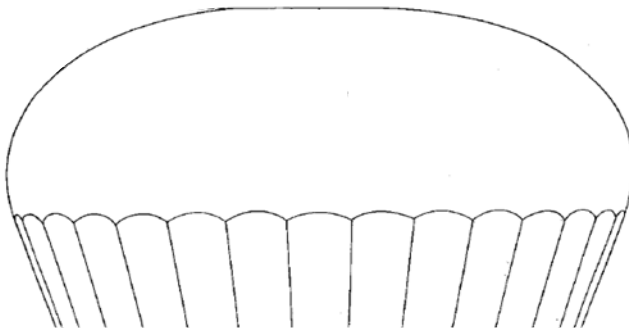


**Figure 2. Woven straps forming filamentary pressure vessel with state of the art opening.**

**Table 1. Hatch component weights. 1.02 m (40 inch) inside diameter.**

	Weight (N)	Weight (lbs)
Hatch Frame	602.4	135.4
Hatch Door Assembly	270.7	60.9
Clevises (62 longitudinal, 94 hoop)	220.7	49.6
Bladder Sealing Rings	54.4	12.2
O-Rings	4.9	1.1
Total	1153.1	259.2

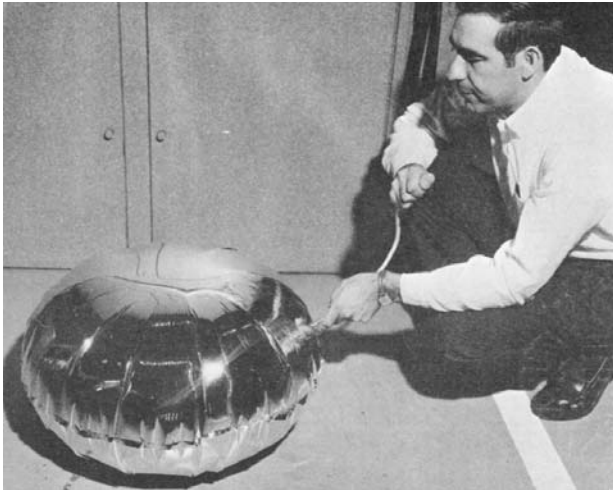


**a) Zero hoop stress parachute shape as originally developed and analyzed by Sir Geoffrey Ingram Taylor in 1919 (ref 2).**

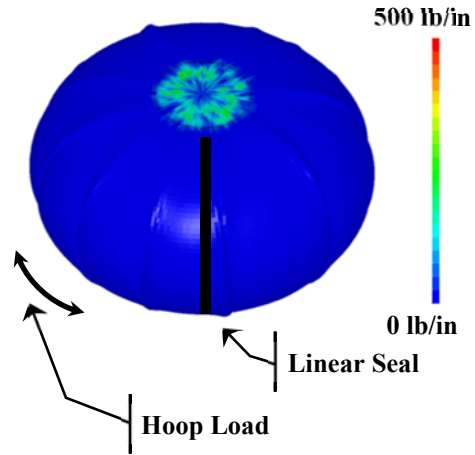


**b) Orion parachute in reefed state.**

**Figure 3. Parachute shape relying on lobed structure to transfer load to cordage.**

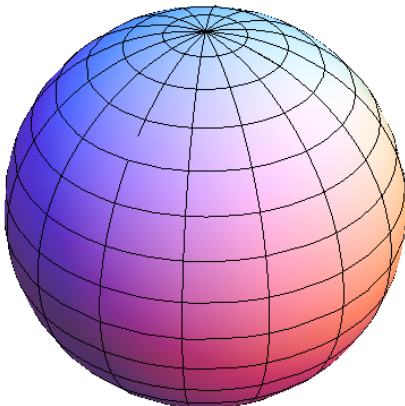


a) Inflation of zero hoop stress shape.



b) Hoop load in zero hoop stress shape and potential location for a linear seal.

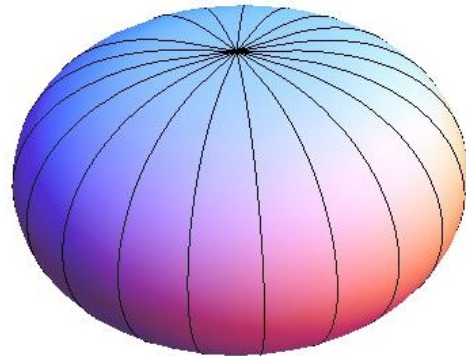
Figure 4. Zero hoop stress test article developed and analyzed by Mikulas in 1970 (ref 1).



**Features**

- Equal stress (load) in both directions
- Ideal for isotropic material
- Fibers required in two directions for composite material
- Hoop fibers not on geodesics

a) Sphere.



**Features**

- Stress (load) only in meridional direction
- Ideal for composite material
- All fibers on geodesics

b) Zero hoop stress shape.

Figure 5. Typical shapes considered for elongated pressure vessel end domes.

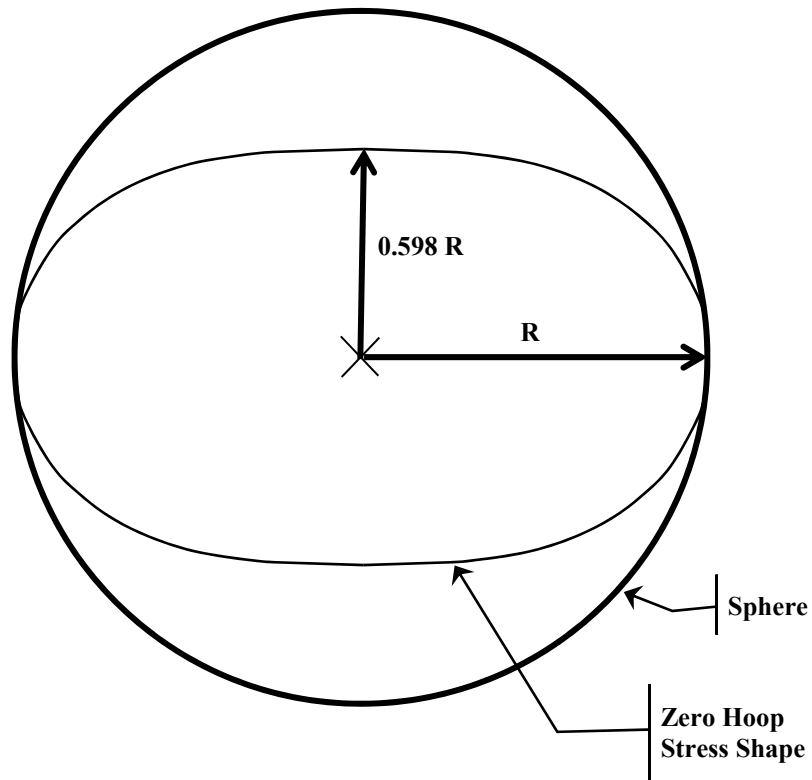


Figure 6. Comparison of the cross-sections of a zero hoop stress shape and sphere with the same maximum radius.

Table 2. Comparison of the geometric properties for a zero hoop stress shape and a sphere of the same radius.

	Sphere	Zero Hoop Stress Shape
Circumference	$2\pi R$	$5.244R$
Cross-section area through poles (figure 6)	$\pi R^2$	$2R^2$
Surface Area	$4\pi R^2$	$7.828R^2$
Volume	$\frac{4}{3}\pi R^3$	$\frac{1}{3}\pi^2 R^3$

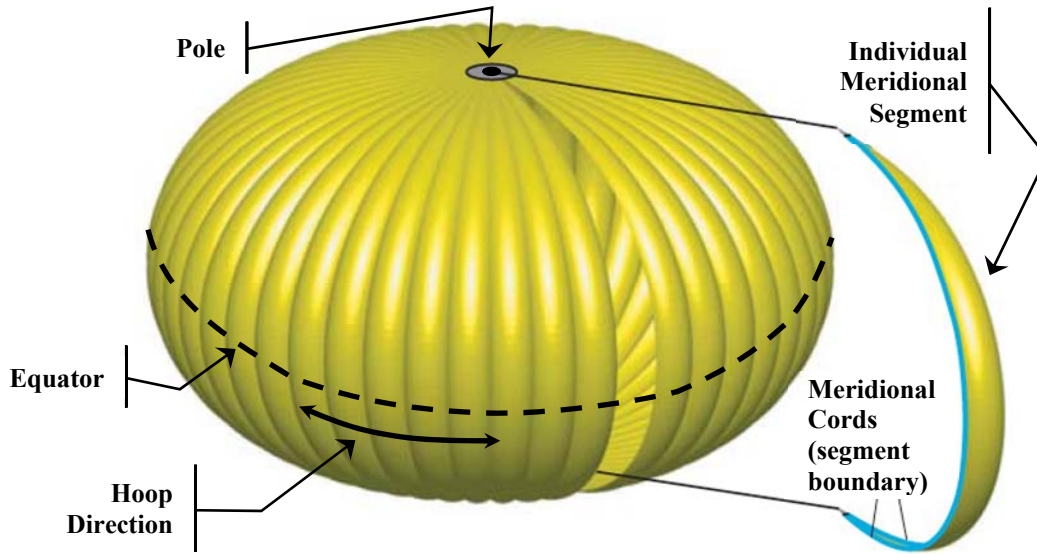


Figure 7. Schematic of a zero hoop stress shape identified by Pagitz and Pellegrino (ref. 9) where the individual meridional segments are in equilibrium with the internal

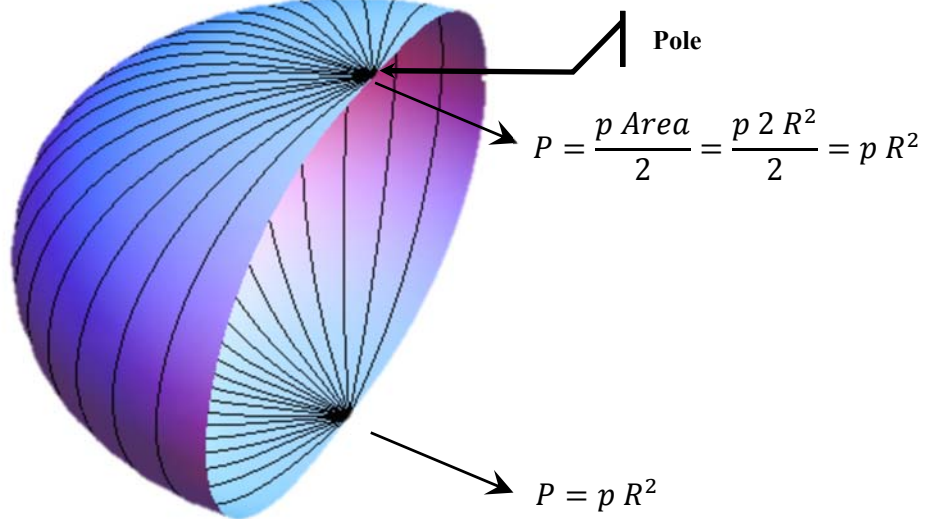


Figure 8. In a zero hoop stress shape, the loads at the poles, P, must resist all the pressure load acting on the cross-sectional area.

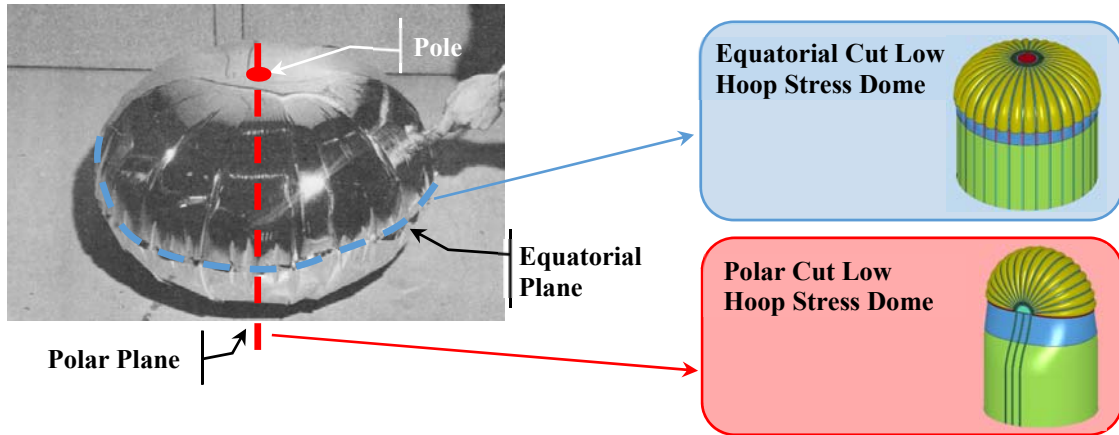
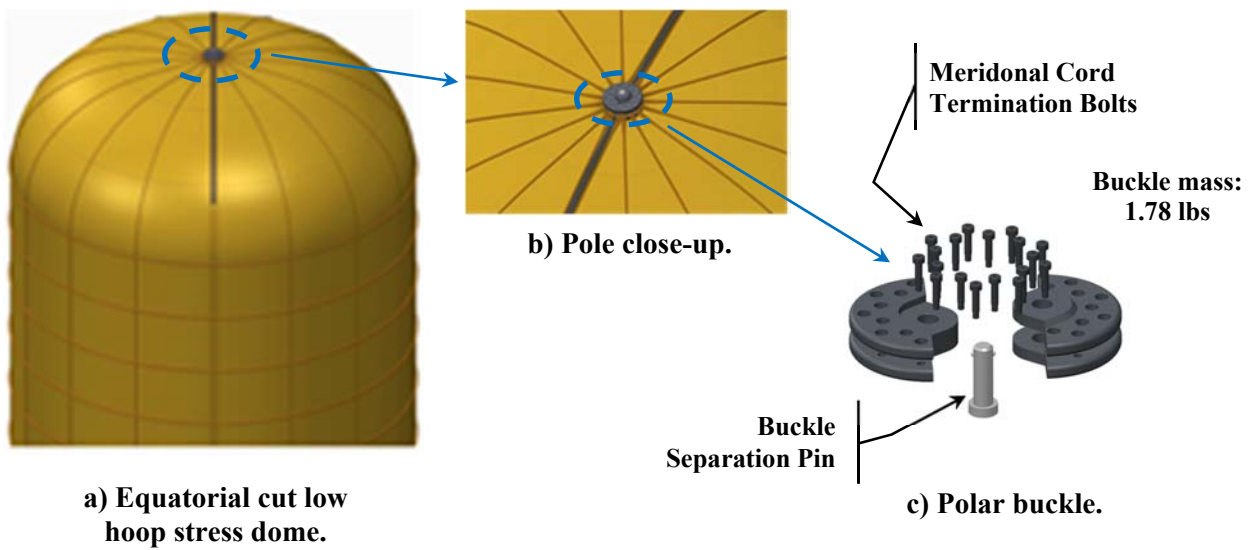


Figure 9. Potential shapes formed from zero hoop stress shape and cylinder mid body.



a) Equatorial cut low hoop stress dome.

b) Pole close-up.

c) Polar buckle.

Figure 10. Polar buckle to allow separation of load carrying elements at pole.

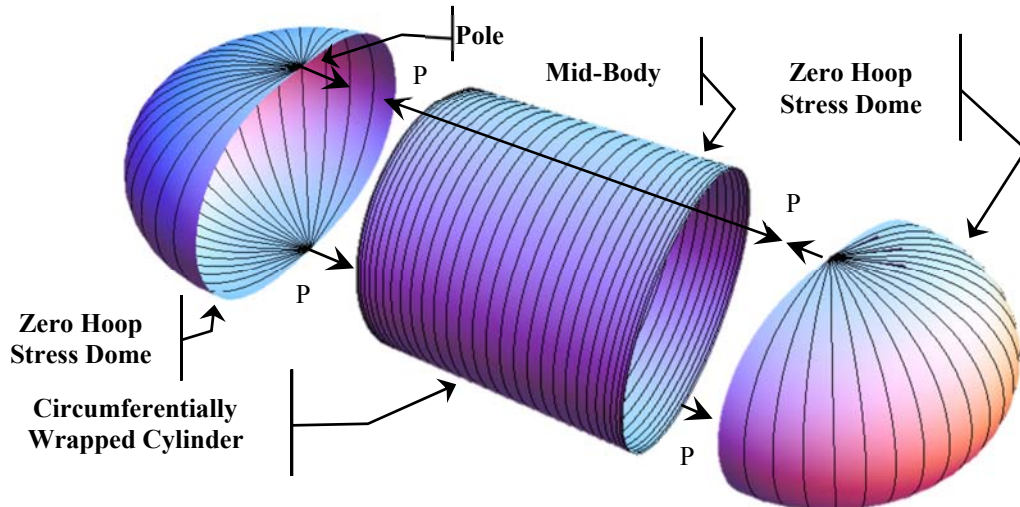


Figure 11. NAIPS consists of two separated halves of a zero hoop stress isotensoid shape joined together by a circumferentially wrapped cylindrical section and two axial cords.

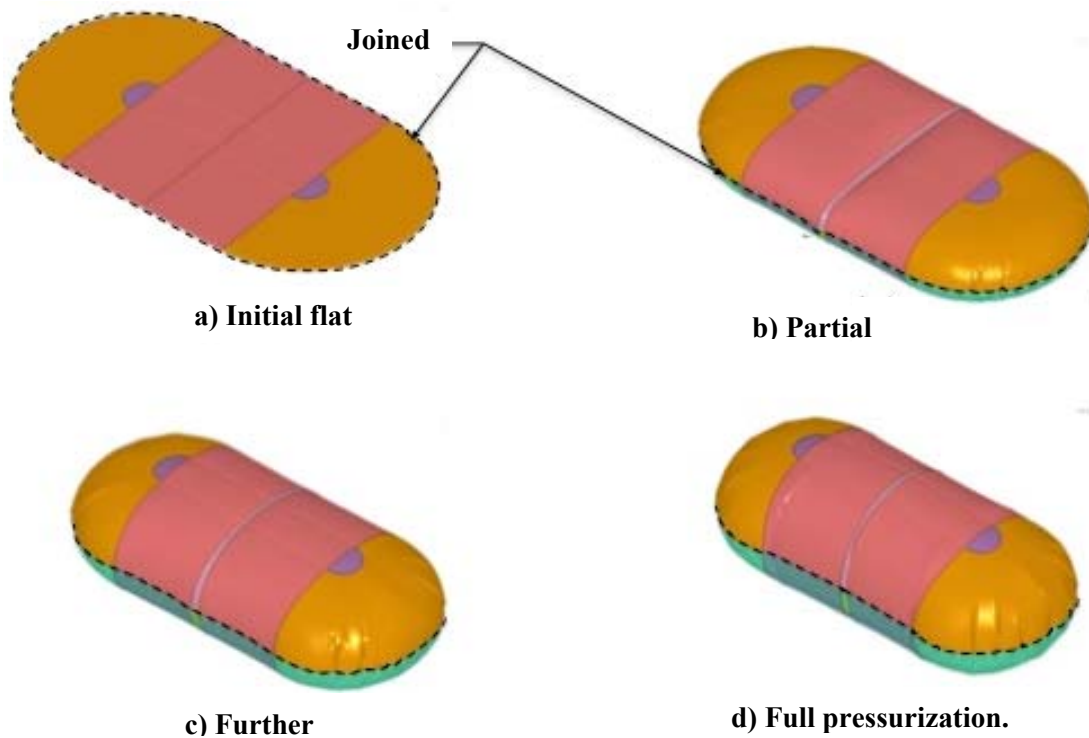
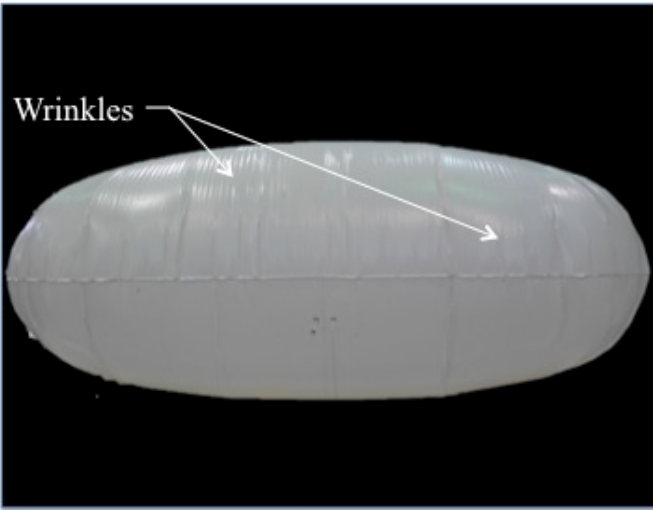


Figure 12. FEA inflation simulation sequence of an elongated airlock fabricated from two flat sheets.



a) Side view.



b) Perspective view.

Figure 13. Full-scale low surface stress polypropylene model of a NAIPS without cords.

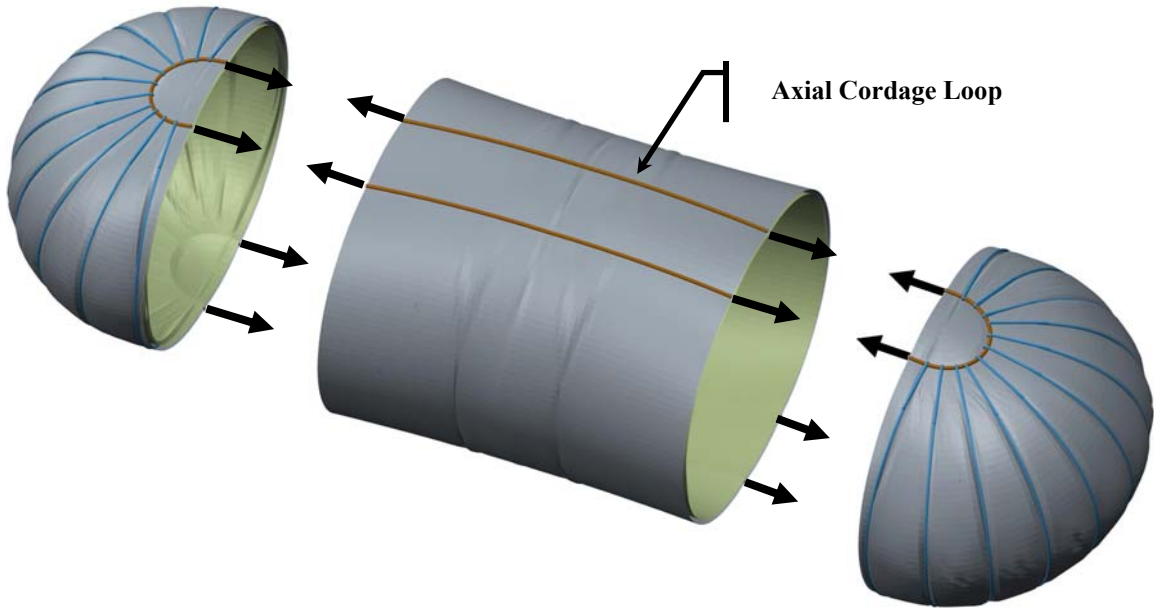
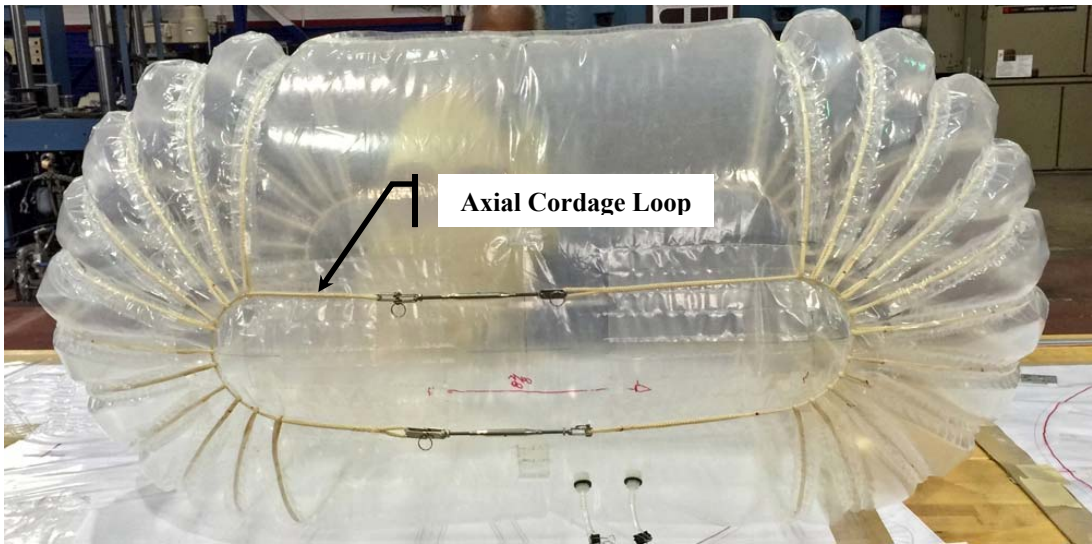


Figure 14. Primary load carrying cords shown on gray schematic of NAIPS.



a) Side view.



b) Top view.

Figure 15. Development model showing the primary load carrying cords.



a) Demonstration model with suited astronauts superimposed.



b) Artist drawing with the hatch opening.

Figure 16. Two views of the full-scale NAIPS airlock concept.

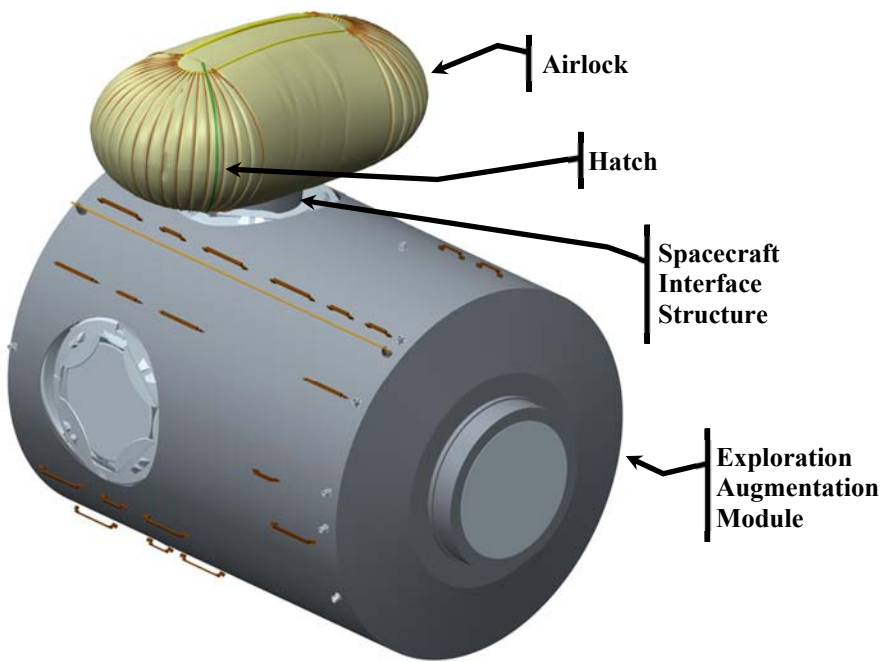
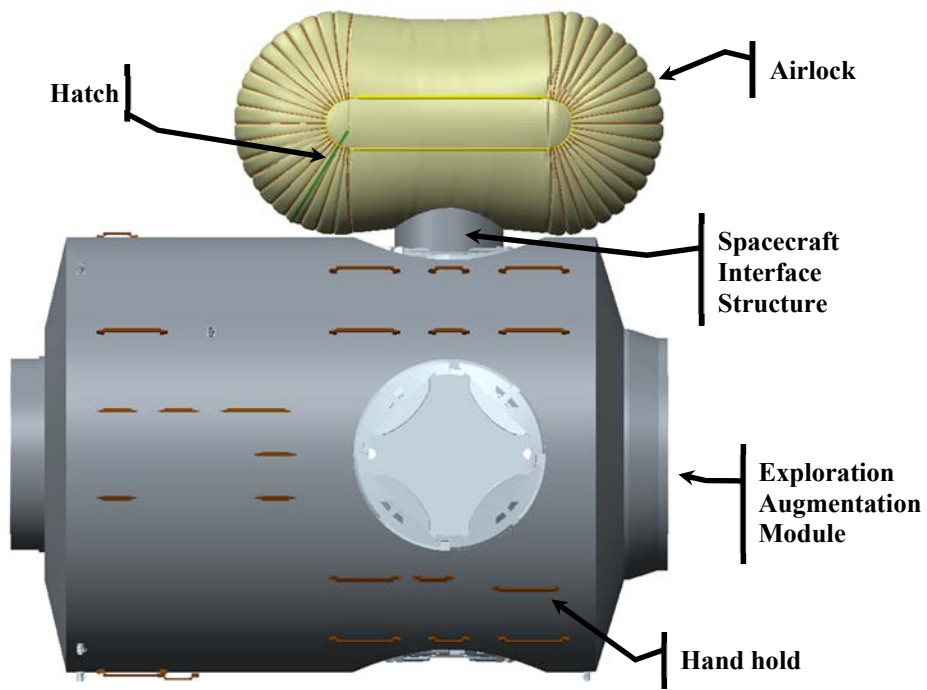


Figure 17. Deployed airlock with entry transition structure from vehicle between axial cords.



**Figure 18. Deployed airlock with equatorial interface for entry transition structure.**

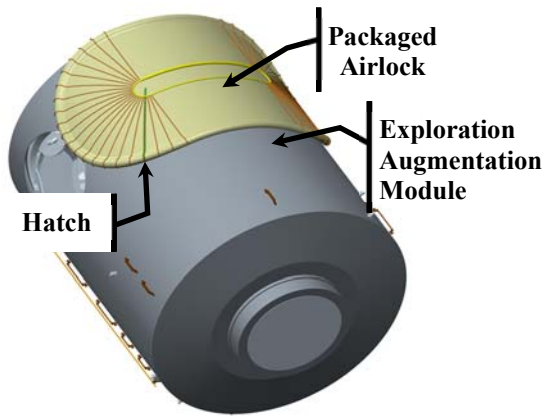


Figure 19. Packaged airlock with entry transition structure between axial cords.

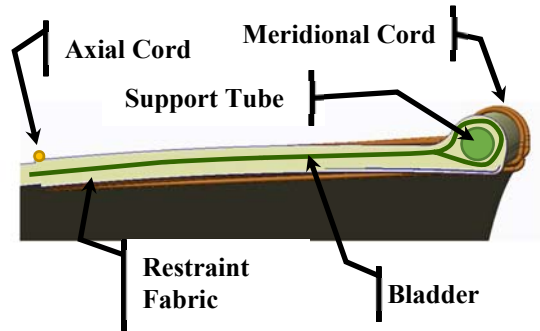


Figure 20. Folding of the seal forming hatch.

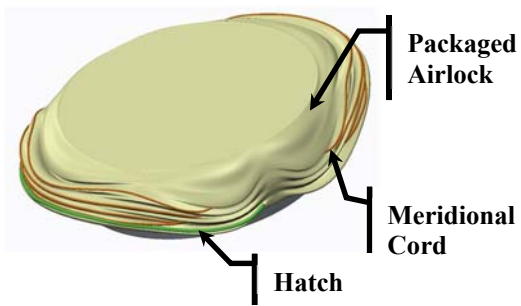


Figure 21. Packaged airlock with equatorial entry transition structure.

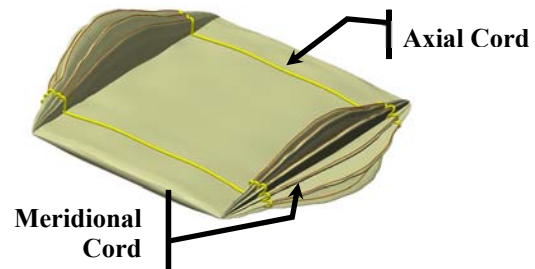
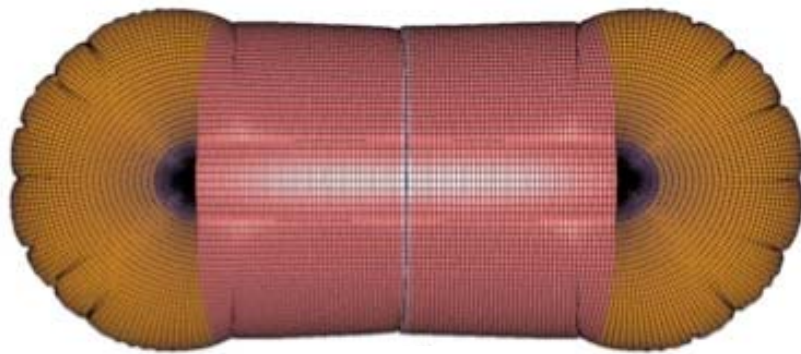
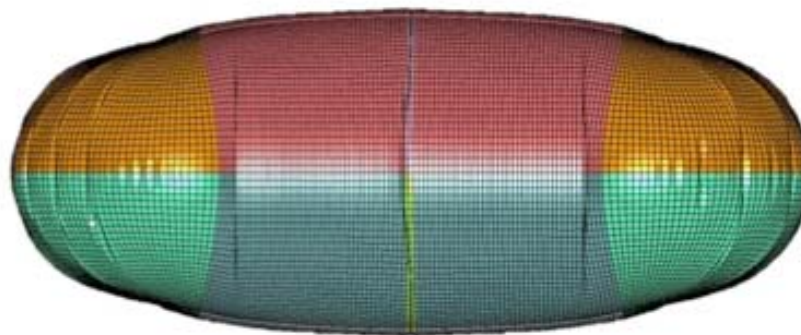


Figure 22. Packaging start for equatorial hatch.



a) Top view.



b) Side view.

Figure 23. FEA model of NAIPS.

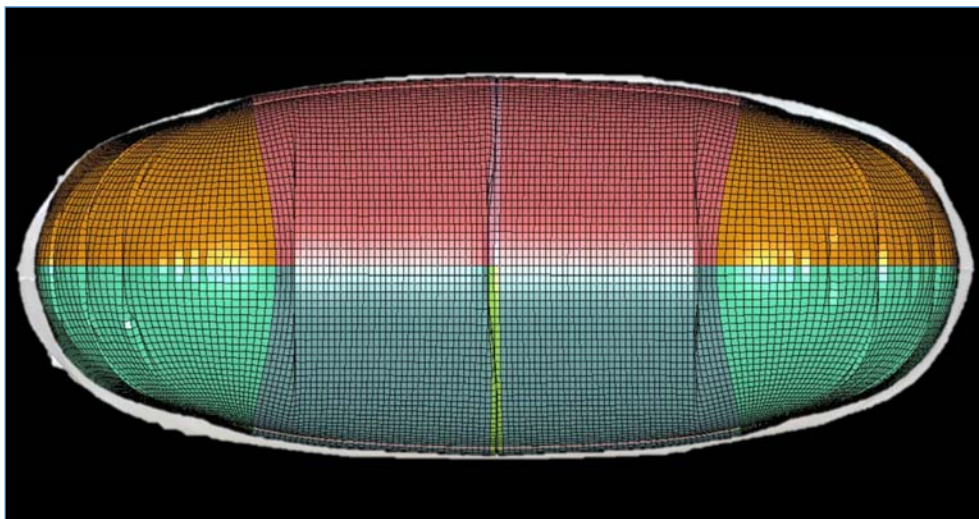
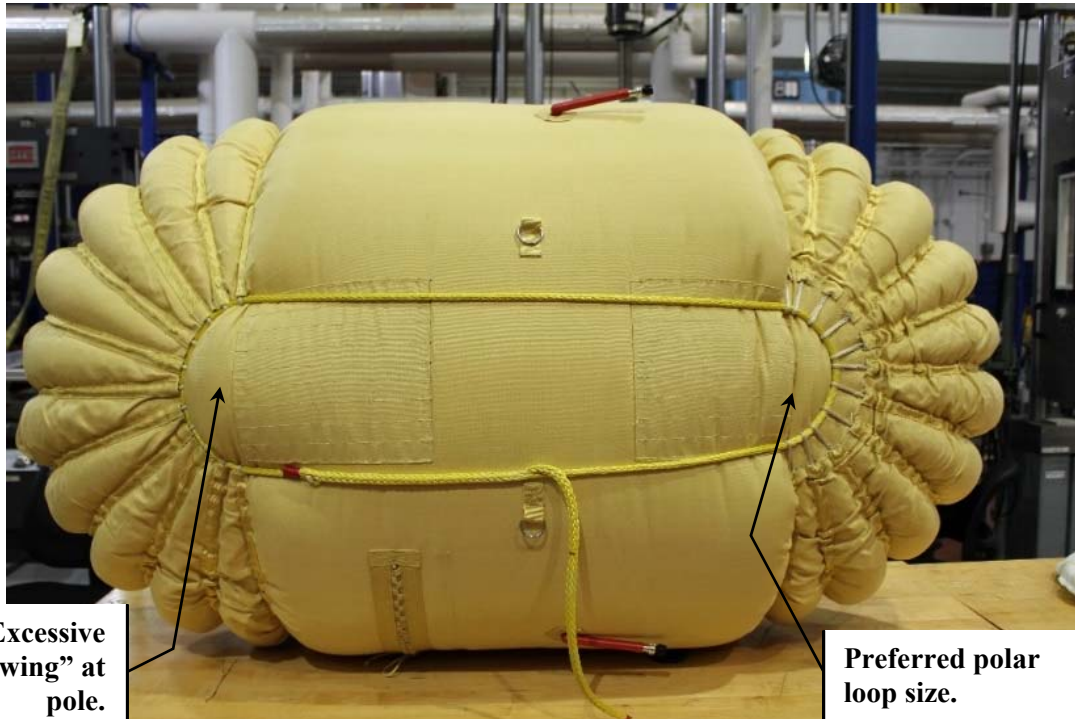


Figure 24. FEA model of NAIPS superimposed upon the polypropylene model.



a) Side view.

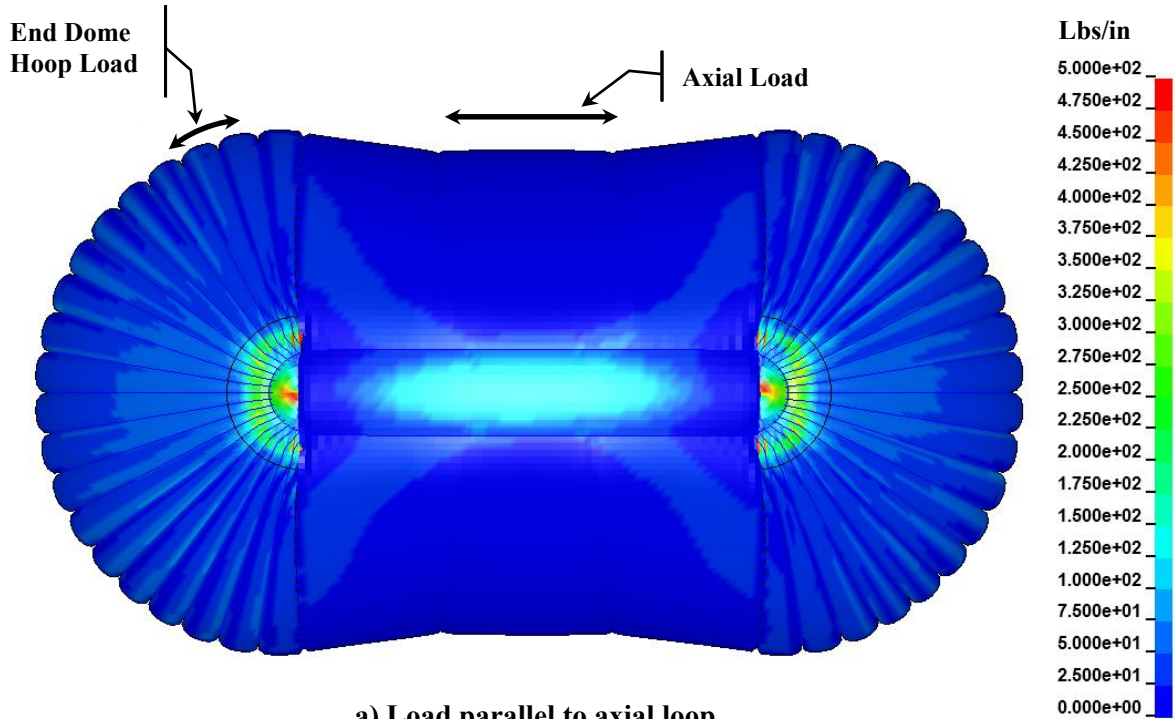


Excessive  
"pillowing" at  
pole.

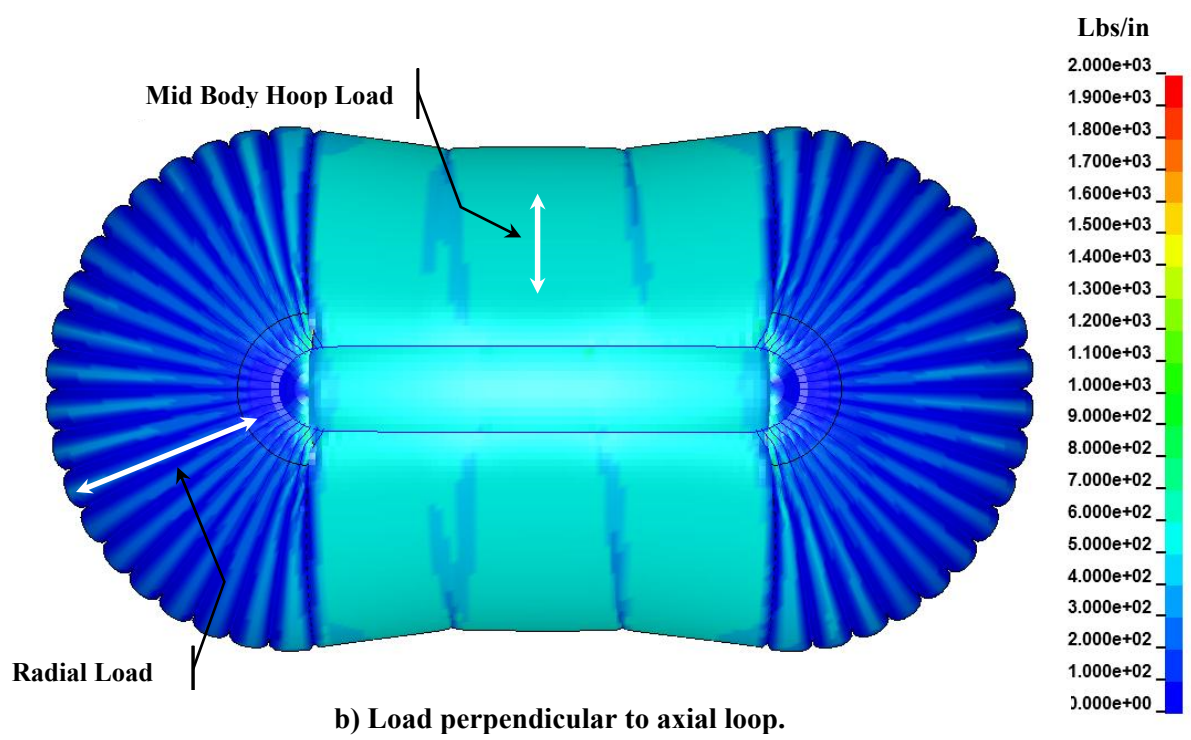
Preferred polar  
loop size.

a) Top view.

Figure 25. 3/8th scale Kevlar model used to refine meridional tendon geometry.



a) Load parallel to axial loop.



b) Load perpendicular to axial loop.

Figure 26. Line loads in full scale 21 lobe FEA.

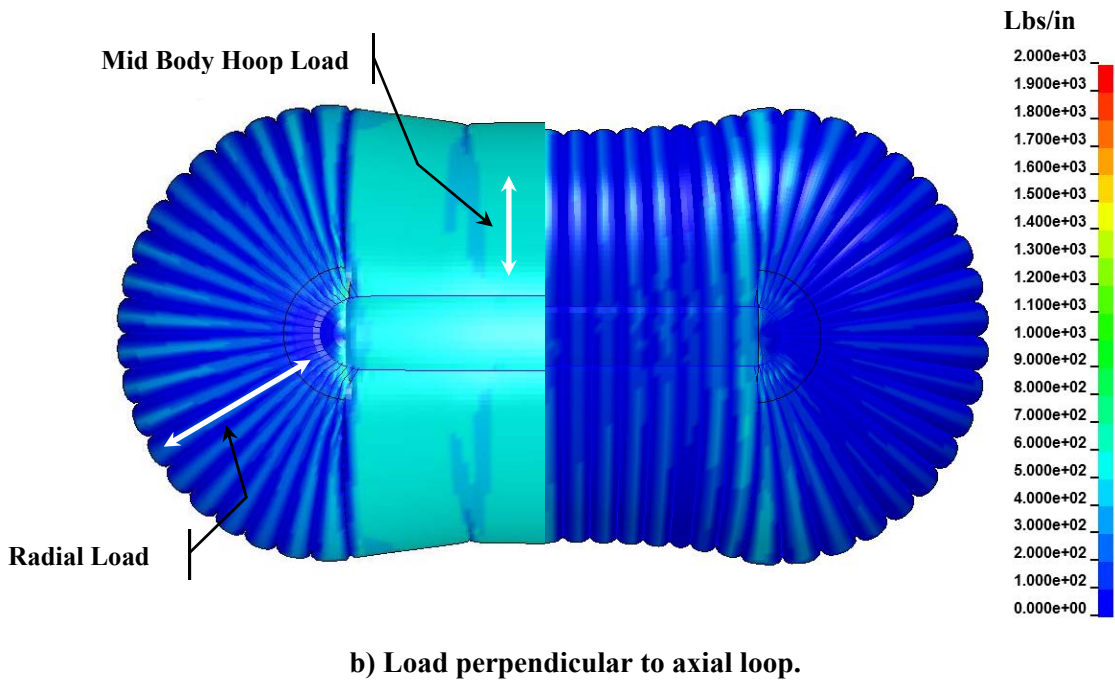
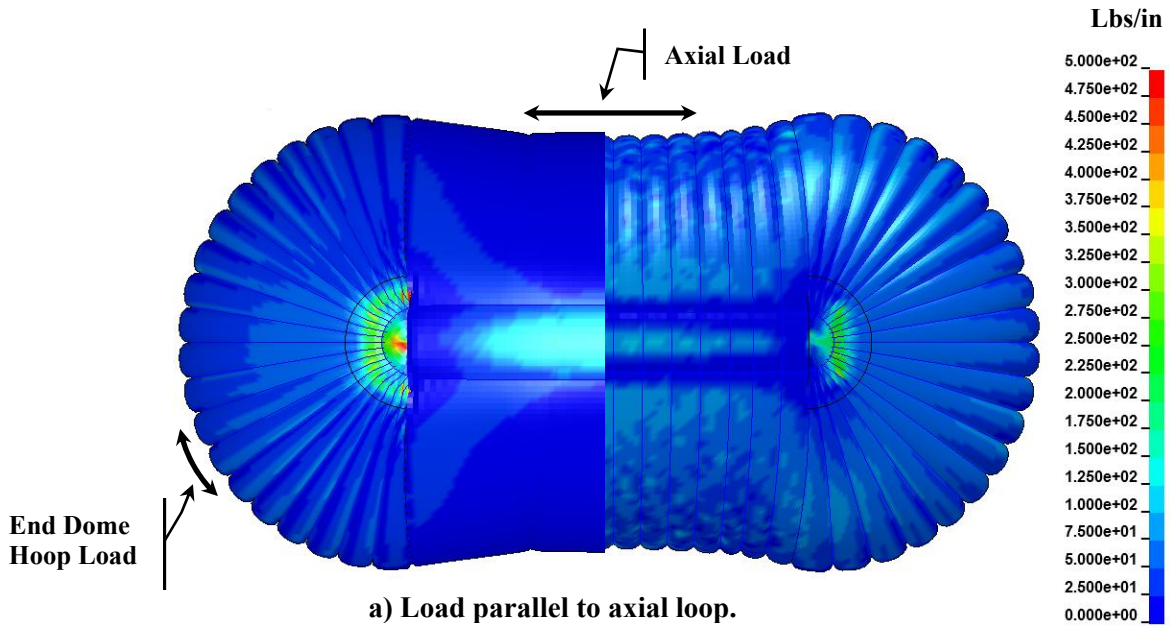


**Figure 27. FEA comparison of 21 lobe dome with and without mid-body lobes generated by adding mid-body grommets.**

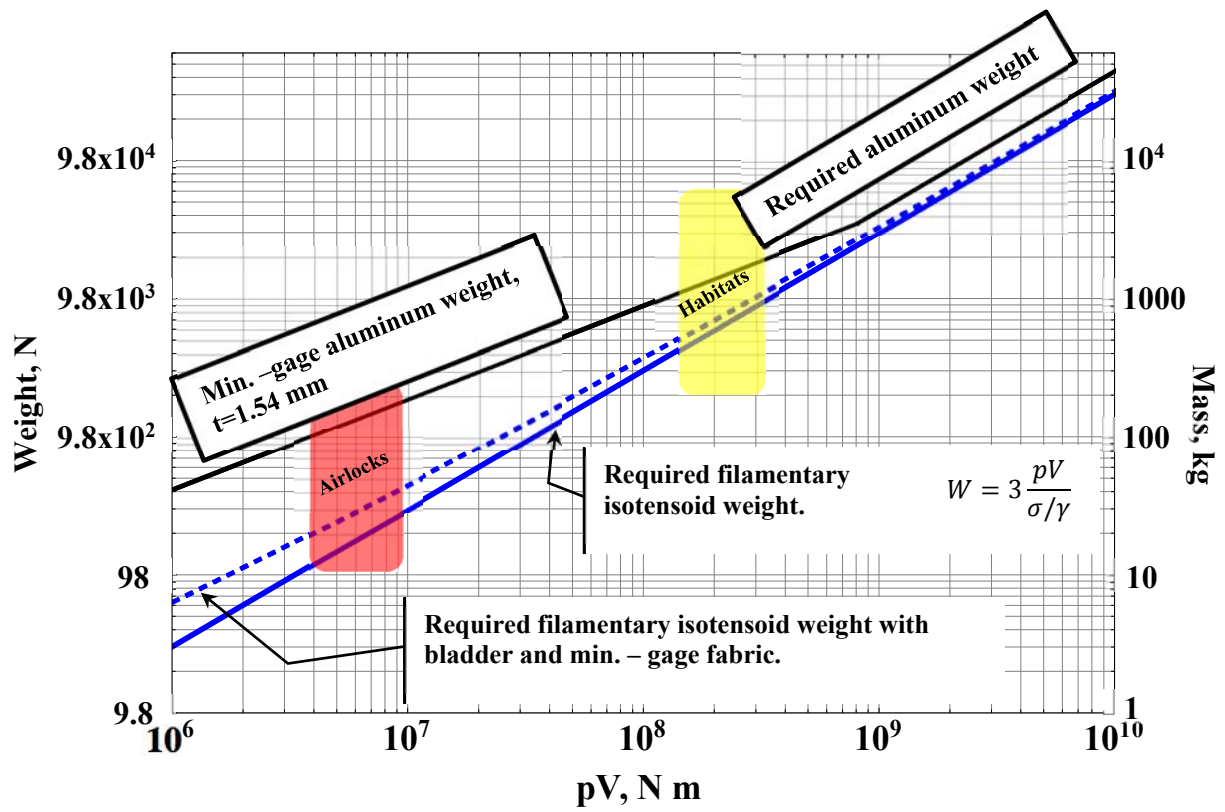


Figure 28. Weight performance metric chart enabling weight projections at different scales (SI units).

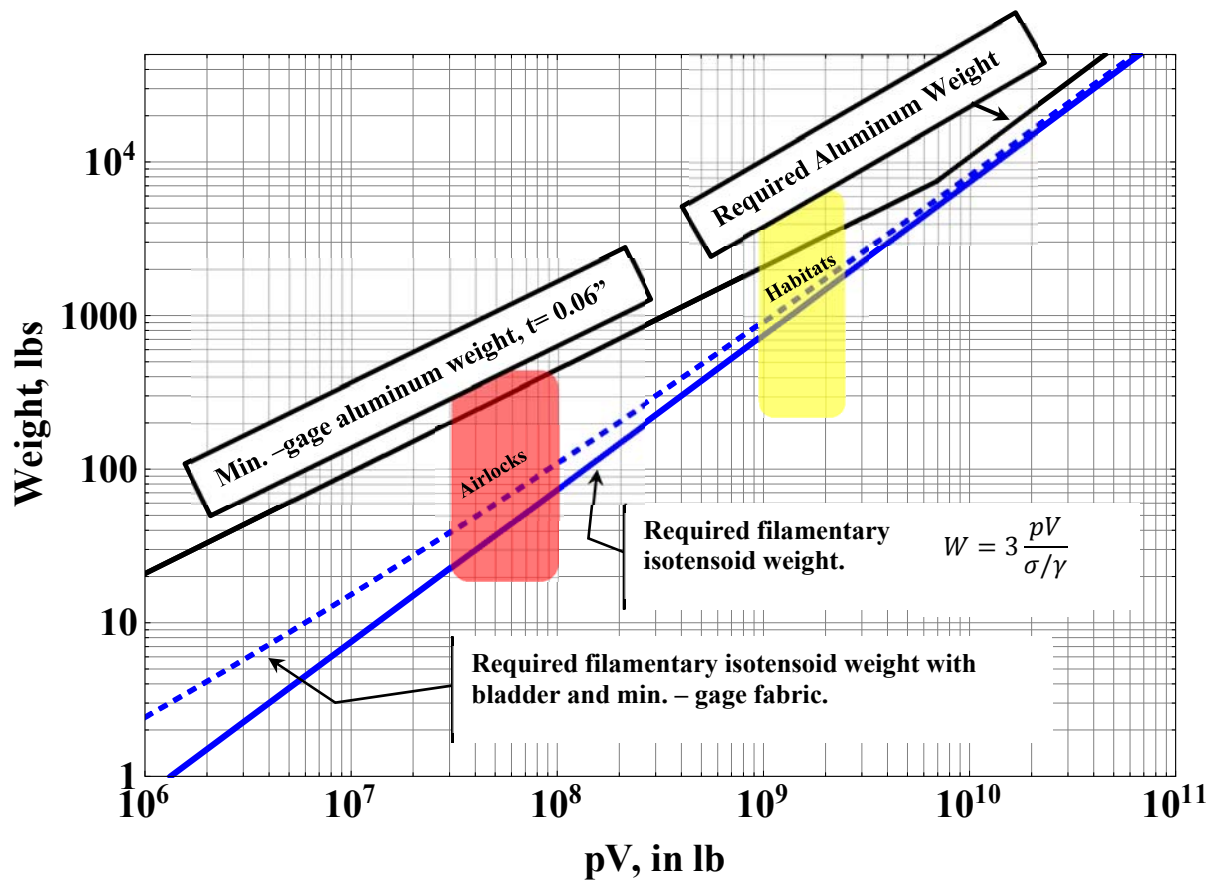


Figure 29. Weight performance metric chart enabling weight projections at different scales in (English units).

Table 3. Material properties for figures 28 and 29.

Vect	ran		Aluminum		Bladder+Lobed Fabric	
	Maximum Stress ( $\sigma$ )	200 ksi	1,379 Mpa	83 ksi	572 MPa	NA
Specific Weight ( $\gamma$ )	0.05 lb/in <sup>3</sup>	13.7 kN/m <sup>3</sup>	0.1 lb/in <sup>3</sup>	27.5 kN/m <sup>3</sup>	0.04 lb/in <sup>3</sup>	11 kN/m <sup>3</sup>
Specific Strength ( $\sigma/\gamma$ )	$4 \times 10^6$ in	102 km	$8.3 \times 10^5$ in	21.1 km	NA	
Minimum gage	NA	NA	0.06 in	1.54 mm	0.012 in	0.3 mm

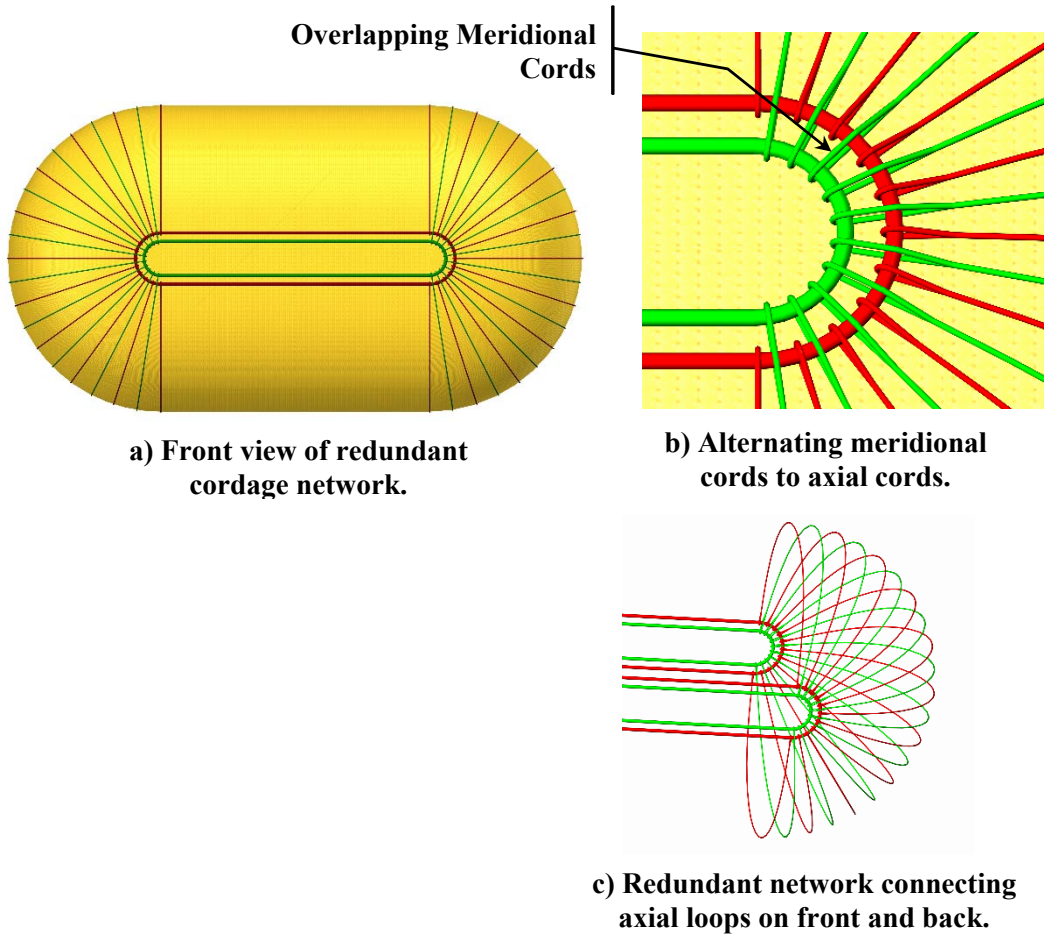


Figure 30. NAIPS with redundant cordage network.

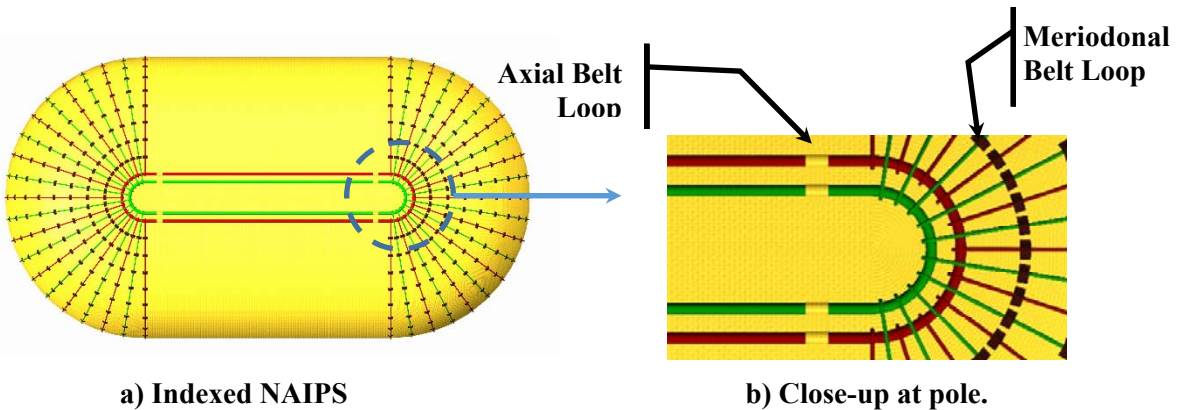


Figure 31. NAIPS with redundant cordage network indexed to fabric layer.

**REPORT DOCUMENTATION PAGE**

Form Approved  
OMB No. 0704-0188

The public reporting burden for this collection of information is estimated to average 1 hour per response, including the time for reviewing instructions, searching existing data sources, gathering and maintaining the data needed, and completing and reviewing the collection of information. Send comments regarding this burden estimate or any other aspect of this collection of information, including suggestions for reducing the burden, to Department of Defense, Washington Headquarters Services, Directorate for Information Operations and Reports (0704-0188), 1215 Jefferson Davis Highway, Suite 1204, Arlington, VA 22202-4302. Respondents should be aware that notwithstanding any other provision of law, no person shall be subject to any penalty for failing to comply with a collection of information if it does not display a currently valid OMB control number.  
**PLEASE DO NOT RETURN YOUR FORM TO THE ABOVE ADDRESS.**

<b>1. REPORT DATE (DD-MM-YYYY)</b> 01-08-2016		<b>2. REPORT TYPE</b> Technical Memorandum		<b>3. DATES COVERED (From - To)</b>	
<b>4. TITLE AND SUBTITLE</b>  Non-Axisymmetric Inflatable Pressure Structure (NAIPS) Concept that Enables Mass Efficient Packageable Pressure Vessels with Sealable Openings				<b>5a. CONTRACT NUMBER</b>	
				<b>5b. GRANT NUMBER</b>	
				<b>5c. PROGRAM ELEMENT NUMBER</b>	
				<b>5d. PROJECT NUMBER</b>	
<b>6. AUTHOR(S)</b>  Doggett, William R.; Jones, Thomas C.; Kenner, Winfred S.; Moore, David F.; Watson, Judith J.; Warren, Jerry E.; Makino, Alberto; Yount, Bryan; Selig, Molly; Shariff, Khadijah; Litteken, Douglas; Mikulas, Martin M., Jr.				<b>5e. TASK NUMBER</b>	
				<b>5f. WORK UNIT NUMBER</b>  432938.11.01.07.43.40.12	
				<b>8. PERFORMING ORGANIZATION REPORT NUMBER</b>  L-20730	
<b>7. PERFORMING ORGANIZATION NAME(S) AND ADDRESS(ES)</b>  NASA Langley Research Center Hampton, VA 23681-2199				<b>10. SPONSOR/MONITOR'S ACRONYM(S)</b>  NASA	
<b>9. SPONSORING/MONITORING AGENCY NAME(S) AND ADDRESS(ES)</b>  National Aeronautics and Space Administration Washington, DC 20546-0001				<b>11. SPONSOR/MONITOR'S REPORT NUMBER(S)</b> NASA-TM-2016-219331	
				<b>12. DISTRIBUTION/AVAILABILITY STATEMENT</b>  Unclassified - Unlimited Subject Category 39 Availability: NASA STI Program (757) 864-9658	
<b>13. SUPPLEMENTARY NOTES</b>					
<b>14. ABSTRACT</b> Achieving minimal launch volume and mass are always important for space missions, especially for deep space manned missions where the costs required to transport mass to the destination are high and volume in the payload shroud is limited. Pressure vessels are used for many purposes in space missions including habitats, airlocks, and tank farms for fuel or processed resources. A lucrative approach to minimize launch volume is to construct the pressure vessels from soft goods so that they can be compactly packaged for launch and then inflated en route or at the final destination. In addition, there is the potential to reduce system mass because the packaged pressure vessels are inherently robust to launch loads and do not need to be modified from their in-service configuration to survive the launch environment. A novel concept is presented herein, in which sealable openings or hatches into the pressure vessels can also be fabricated from soft goods. To accomplish this, the structural shape is designed to have large regions where one principal stress is near zero. The pressure vessel is also required to have an elongated geometry for applications such as airlocks.					
<b>15. SUBJECT TERMS</b>  Concept; Inflatable pressure structure; Non-Axisymmetric; Pressure vessels					
<b>16. SECURITY CLASSIFICATION OF:</b>			<b>17. LIMITATION OF ABSTRACT</b>	<b>18. NUMBER OF PAGES</b>	<b>19a. NAME OF RESPONSIBLE PERSON</b>
<b>a. REPORT</b>	<b>b. ABSTRACT</b>	<b>c. THIS PAGE</b>			STI Help Desk (email: help@sti.nasa.gov)
U	U	U	UU	42	<b>19b. TELEPHONE NUMBER (Include area code)</b> (757) 864-9658